Society for
Mathematical
Biology

ORIGINAL ARTICLE

Modelling ion channels with a view towards identifiability

Ivo Siekmann[1] ⓘ

Abstract
Aggregated Markov models provide a flexible framework for stochastic dynamics that develops on multiple timescales. For example, Markov models for ion channels often consist of multiple open and closed state to account for "slow" and "fast" openings and closings of the channel. The approach is a popular tool in the construction of mechanistic models of ion channels—instead of viewing model states as generators of sojourn times of a certain characteristic length, each individual model state is interpreted as a representation of a distinct biophysical state. We will review the properties of aggregated Markov models and discuss the implications for mechanistic modelling. First, we show how the aggregated Markov models with a given number of states can be calculated using Pólya enumeration. However, models with n_O open and n_C closed states that exceed the maximum number $2n_O n_C$ of parameters are non-identifiable. We will present two derivations of this classical result and investigate non-identifiability further via a detailed analysis of the non-identifiable fully connected three-state model. Finally, we will discuss the implications of non-identifiability for mechanistic modelling of ion channels. We will argue that instead of designing models based on assumed transitions between distinct biophysical states which are modulated by ligand binding, it is preferable to build models based on additional sources of data that give more direct insight into the dynamics of conformational changes.

Keywords Non-identifiability · Aggregated Markov model · Ion channel

1 Introduction

Ion channels belong to the simplest components of living cells—in membranes that are usually impermeable to ions they open tiny pores which allow ions to enter or leave the cell. Many channels select which ions can pass through the pore but otherwise, ion channels exert little influence on the net flux of ions which is determined

---

Dedicated to Edmund J. Crampin (1973-2021).

✉ Ivo Siekmann
  i.siekmann@ljmu.ac.uk

1   School of Computer Science and Mathematics (CSM), Liverpool John Moores University (LJMU),
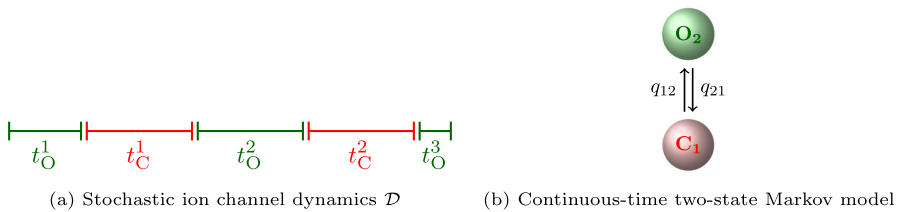   Byrom Way, Liverpool L3 3AF, Merseyside, United Kingdom

⊘ Springer

(a) Stochastic ion channel dynamics $\mathcal{D}$ (b) Continuous-time two-state Markov model

Fig. 1 (a) The dynamics $\mathcal{D}$ of an ion channel is an alternating sequence of stochastic open and closed times t_O^i and t_C^j. (b) Such a sequence can be described by a continuous-time Markov model with one closed state C_1 and one open state O_2. If the ion channel generates open or closed times of multiple characteristic lengths, additional open or closed states need to be added.

by a combination of the concentration gradient and the membrane potential i.e. the electrochemical gradient. Thus, at the most basic level, ion channels can be viewed as switches which are able to switch on or off fluxes of ions that would otherwise be blocked by the cell membrane.

Despite, or maybe due to their simplicity which enables them to be flexibly integrated in various physiological systems, ion channels are involved in more or less all important physiological processes. These can be roughly summarised in three categories:

1. Regulating the intracellular concentration of a particular ion.
2. Regulating the charge within a cell i.e. the membrane potential.
3. Signal transduction.

Ion channels belong to a class of cellular building blocks called membrane proteins. Although the function carried out by an ion channel can be described as one of a simple switch, the membrane protein which carries out this task is not at all simple at a biophysical level—to open a pore in the membrane, the channel protein needs to undergo one or more rearrangements of its complex three-dimensional structure—so-called conformational changes.

A fundamental question in ion channel modelling is

"Should the *biophysics of the channel protein* be reflected in a mathematical model describing the *dynamics of the ion channel*?"

We initially disregard this important question but will return to consider it after our detailed investigation of non-identifiability, see the Discussion, sec. 4.

We describe the dynamics $\mathcal{D}$ of an ion channel as an alternating sequence of open and closed times, $\mathcal{D} = \left(t_O^1, t_C^1, t_O^2, t_C^2, \dots \right)$ (Without loss of generality we assume that the first time observed is an open time but we could equally have started with a closed time). The times $t_O^1, t_C^1, \dots$ are stochastic—when an ion channel opens, it is, in principle, not possible to predict, how long it will stay open, see Fig. 1.

A simple model for the alternating sequence of open and closed times $\mathcal{D}$ is the two-state continuous-time Markov model which describes stochastic transitions between a closed state C_1 and an open state O_2. A direct consequence of assuming that the dynamics $\mathcal{D}$ can be described by a Markov model is that the open times t_O^i and the

closed times t_C^j are exponentially-distributed. Indeed, the Markov property requires that if the model has been in a state S for a time t_0, the probability that it stays in this state for an additional duration τ is independent from the time t_0 that has already passed. More formally,

$$\mathbb{P}(T > \tau + t_0) = \mathbb{P}(T > t_0)\mathbb{P}(T > \tau), \quad t_0 \geq 0, \tau \geq 0 \tag{1}$$

or, equivalently,

$$\mathbb{P}(T > \tau + t_0 | T > t_0) = \mathbb{P}(T > \tau), \quad t_0 \geq 0, \tau \geq 0. \tag{2}$$

The exponential distribution is the only continuous-time distribution for which the "lack of memory" property (2) holds. A two-state Markov model can therefore just generate an alternating sequence of exponentially-distributed sequence of open and closed times. But exponentially-distributed open and closed time distributions, $f_O(t_O)$ and $f_C(t_C)$, are insufficient for describing the dynamics $\mathcal{D}$ of many ion channels—a simple counter-example is an ion channel that sometimes stays closed for a short time and sometimes for a considerably longer time. The most common approach for describing multiple timescales in the open and closed time distributions is to introduce multiple open and closed states. Intuitively, one might expect that each closed state (or open state) represents a different exponentially distributed timescale and each of these closed (or open) timescales is observed with a specific probability. Indeed, as calculating the sojourn-time distributions from a Markov model (with an arbitrary number of closed and open states) shows, this expectation turns out to be true—open and closed time distributions are mixture distributions of as many exponential components as there are open/closed states, respectively (Colquhoun and Hawkes 1981). Although the exponentials in the mixture distributions $f_O(t_O)$ and $f_C(t_C)$ can, in general, not be identified with individual states in the Markov model, it is tempting to interpret the set of open and closed states as a collection of different timescales, ranging from "slow" to "fast".

Another attractive property of a Markov model consisting of multiple open and closed states (a so-called *aggregated Markov model* with two classes) is that one might associate individual states of the model with different biophysical states of the channel protein—one well-known example is the de Young - Keizer model of the inositol-trisphosphate receptor (IP$_3$R) (De Young and Keizer 1992). To give a simple example for this approach, consider a model that consists of a chain of multiple closed states that eventually transition to an open state, this is interpreted as transitions between various closed conformations which eventually lead to an open state i.e. a conformation in which the channel is open.

It is no coincidence that this idea has been highly influential—it suggests that a model consisting of multiple open and closed states can represent more than "just" the opening and closing of an ion channel but, in addition, can reveal the hidden dynamics of conformational changes underlying these dynamics $\mathcal{D}$. For a given number of open and closed states, n_O and n_C, there are many different ways that these states can be connected to an aggregated Markov model, see Section 2 for an explicit calculation, the results are summarised in Table 1. Intuitively, it seems plausible that for a given number

of open and closed states, any of the different models represent different dynamics $\mathcal{D}$. A review of long-known results on aggregated Markov models shows that this intuition turns out to be clearly wrong, as we will explain in Section 3—models with n_O open and n_C closed states can be reparametrised without altering the dynamics $\mathcal{D}$. For example, the fully-connected model for any number of states $n_O + n_C > 2$ can be continuously reparametrised so that an infinite combination of parameters can represent the same dynamics.

The phenomenon that a given model Q can be reparametrised to a different model Q' that represents the dynamics $\mathcal{D}$ equally well is known as non-identifiability. We will consider two different aspects of this question:

1. For a given Markov model $Q = (q_{ij})$ with n_O open and n_C closed states, can the rate constants q_{ij} be uniquely identified from the dynamics $\mathcal{D}$? If this is the case, the model Q is referred to as *parameter-identifiable*.
2. We now consider the *model structure* i.e. the graph $\mathcal{G}$ defined by the positive rates of an infinitesimal generator $Q = (q_{ij})$. We ask the question if Q can be reparametrised to another model Q' so that they generate the same dynamics $\mathcal{D}$ with a model structure $\mathcal{G}'$ that is not equivalent to $\mathcal{G}$ as a graph (by symmetries as described in Section 2). We call two models with generators Q and Q' *equivalent* if they produce the same dynamics $\mathcal{D}$ despite being defined on different graphs $\mathcal{G}$ and $\mathcal{G}'$. If the dynamics $\mathcal{D}$ can be generated by models defined on graphs $\mathcal{G}$ and $\mathcal{G}'$ that are not equivalent we refer to this phenomenon as *non-identifiability of model structure*.

Since the seminal papers by Fredkin et al. (1985); Fredkin and Rice (1986) it has been known that models exceeding $2n_O n_C$ rate constants can, in principle, be reparametrised as in 1. i.e. these models lack parameter identifiability. We provide an outline of the derivation of this result by Fredkin et al. (1985); Fredkin and Rice (1986) in Section 3.1 as well as an alternative derivation in Section 3.2. As a consequence, we might restrict ourselves to models with fewer rate constants than this upper bound $2n_O n_C$. But even models with rate constants below this bound can often be reparametrised to models that have the same number of rate constants but whose states are connected in a different way (these models lack identifiability of model structure as in 2.)—explicit examples are presented in detail in Section 3.4. This means that even in the best case that models cannot be continuously reparametrised, there still is an equivalence class of a finite number of models that represents the same dynamics $\mathcal{D}$. This makes it challenging to interpret aggregated Markov models as representations of a particular biophysical mechanism—simply, because via reparametrisation, the dynamics of a given model can be generated by a different model that suggests a completely different mechanism.

We will then explore the implications of this non-identifiability of model structure on models that are based on representations of transitions between conformational states regulated by ligand binding sites in Section 3.5.

In the light of these difficulties, one might ask the question if aggregated Markov models are a suitable structure for representing the underlying biophysical mechanism of ion channels rather than just the dynamics $\mathcal{D}$. We have argued in Siekmann et al. (2019) that representing biophysical mechanisms such as conformational changes

is unlikely to succeed by parametrising a Markov model from single channel data obtained at steady-state ligand conditions alone. Instead, it is more promising to obtain more direct evidence on the biophysical dynamics by statistically analysing modal gating (Ionescu et al. 2007; Siekmann et al. 2014) which is known to be closely linked with conformational changes or using additional data such as the response of the channel to rapid changes of ligand concentrations (Mak et al. 2007). In the Discussion (Section 4) we will explain how hierarchical Markov models Siekmann et al. (2016) and Markov models with distributed delay (Hawker et al. 2025) can be used for representing aspects of the underlying biophysical dynamics of the channel protein by providing structures that can be parametrised directly with these additional data sources.

2 Enumeration of ion channel models

In Bruno et al. (2005), the number of graphs with n_O open and n_C closed states has been stated (and credited to David Torney) but further information about the derivation of these numbers have not been given. Here, the calculation of the number of graphs is explained. To illustrate the challenge we show a few examples of graphs that are equivalent, although this is not obvious at first glance, see Figure 2.

2.1 Pólya enumeration

We will "count" the number of different graphs using a technique called *Pólya enumeration*[1]. Behind Pólya enumeration is the idea that the number of objects with a particular property can be represented by polynomials $p(t)$.

Let us first look at the very simple example of k-subsets of a set of n elements. If 1 stands for the empty set $\emptyset$ and t for the set $\mathcal{S}_1 = \{1\}$ with one element, the polynomial

$$1 + t \tag{3}$$

represents the two possible subsets with zero and one element. One interpretation of the polynomial $1 + t$ is that we can either draw the (single) element 1 or not.

For the set $\mathcal{S}_2 = \{1, 2\}$ we can extend this idea by considering the product

$$\underbrace{(1+t)}_{\text{draw 1?}} \cdot \underbrace{(1+t)}_{\text{draw 2?}} \tag{4}$$

where the first factor $(1 + t)$ stands for drawing the element 1 (or not) and the second factor stands for drawing element 2 (or not). It is clear that the polynomial

$$1 \cdot 1 + 1 \cdot t + t \cdot 1 + t \cdot t = 1 + 2t + t^2$$

---

[1] Although not the original developer of the theory, Pólya has been very influential in its popularisation and extension in the seminal article (Pólya 1937).
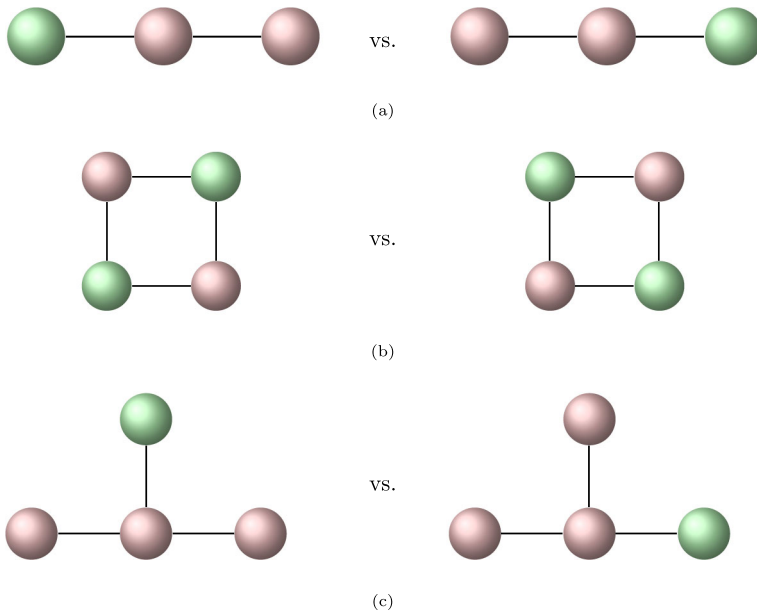
Fig. 2 Three examples of graphs with vertices in two different colours which are equivalent (arguably, with increasing difficulty from (a) to (c)). "Equivalent" means that both are examples of the same unlabelled graph which has just been "drawn" in different ways. More formally, each graph on the left can be mapped to the graph on the right by swapping vertices without changing the adjacency structure. For a given graph which vertices can be mapped to each other is determined by the symmetry group of the graph. Enumeration of graphs with given properties relies on being able to find the symmetry group of this class of graphs and calculating the so-called cycle index, a polynomial which allows to keep track of the different equivalence classes under the operation of the symmetry group.

enumerates all possible outcomes of drawing (without replacement) from $\mathcal{S}_2$. After simplifying the polynomial, the term 1 stands again for the empty set $\emptyset$, $2t$ represents the subsets $\{1\}$ and $\{2\}$ with one element each and t^2 accounts for the full set $\mathcal{S}_2 = \{1, 2\}$ with two elements. Going forward with this idea, for the set $\mathcal{S}_n = \{1, \ldots, n\}$ with n elements, the process of drawing (or not) each of the n elements of the set can be represented via the polynomial

$$(1+t)^n = \underbrace{(1+t)}_{\text{draw 1?}} \cdot \underbrace{(1+t)}_{\text{draw 2?}} \cdots \underbrace{(1+t)}_{\text{draw } n?} \tag{5}$$

and via binomial expansion of (5) we obtain

$$(1+t)^n = \sum_{k=0}^{n} \binom{n}{k} t^k \tag{6}$$

i.e. indeed the coefficient $\binom{n}{k}$ of each term t^k indicates the number of k-subsets in a set with n elements.

In summary, the laws of polynomial arithmetic ensure that all possibilities of drawing k elements from a set with n elements are summarised appropriately.

2.2 Enumerating graphs

We now apply the idea explained in the previous section to a method for calculating the number of unlabelled graphs for a given number of vertices[2]. A graph $\mathcal{G}$ with n_V vertices has a maximal number of $n_\mathrm{E} = \binom{n_\mathrm{V}}{2}$ edges. Similar to the calculation of the k-subsets of the set $\mathcal{S}_n$ with n elements, the idea of enumerating graphs is based on drawing without replacement from the edge set. Unfortunately, the sequence of coefficients $\binom{n_\mathrm{E}}{k}$ of the polynomial $(1+t)^{n_\mathrm{E}}$ does not yield correct results for graphs with more than two vertices. For example, for a graph with $n_\mathrm{V} = 3$ vertices (which has up to $n_\mathrm{E} = 3$ edges), the formula yields $1 + 3t + 3t^2 + t^3$, indicating that there are 3 graphs with one edge and 3 graphs with two edges. This is the correct result for a labelled graph i.e. a graph where any pair of vertices (and thus, also edges between them) can be distinguished from each other. If vertices are not labelled, any rearrangement of vertices that leaves the edge structure of the graph unchanged, is considered to represent the same graph, see Fig. 3.

2.2.1 Symmetry group of a graph—the line group

Because we enumerate graphs by the number n_E of edges we consider the symmetry group on the edge set of the graph, the line group. As an example, the symmetries of a graph with $n_\mathrm{V} = 3$ vertices are shown in Fig. 4.

Each symmetry is a permutation of the edges of the graph and we will represent each permutation via disjoint cycles. Within a cycle $(\cdots)$, each element is mapped to the subsequent element and the last element is mapped to the first one that appears in the cycle (hence the name "cycle"). For example, the cycle (132) maps edge 1 to edge 3, edge 3 to edge 2 and edge 2 to edge 1, see Fig. 4f. The cycle (23) swaps edges 2 and 3, in order to account for what happens to edge 1, we need to add the cycle (1) to account for the fact that edge 1 is left unchanged so that we obtain the cycle representation (1)(23) for the permutation shown in Fig. 4b. It is well-known that any permutation can be represented via *disjoint cycles* i.e. each element appears in any of the cycles exactly once. For a given cycle $(\cdots)$, the number of elements that appear within the cycle are the length of the cycle. For example, the permutation (1)(23) consists of one cycle of length 1 and one cycle of length 2.

2.2.2 The cycle index

The disjoint cycle representation is important because it will help us construct a multivariate polynomial, known as the *cycle index* which will enable us to account for the

---

[2] The application of Pólya enumeration to graphs is presented in the monograph by Harary and Palmer (1973).
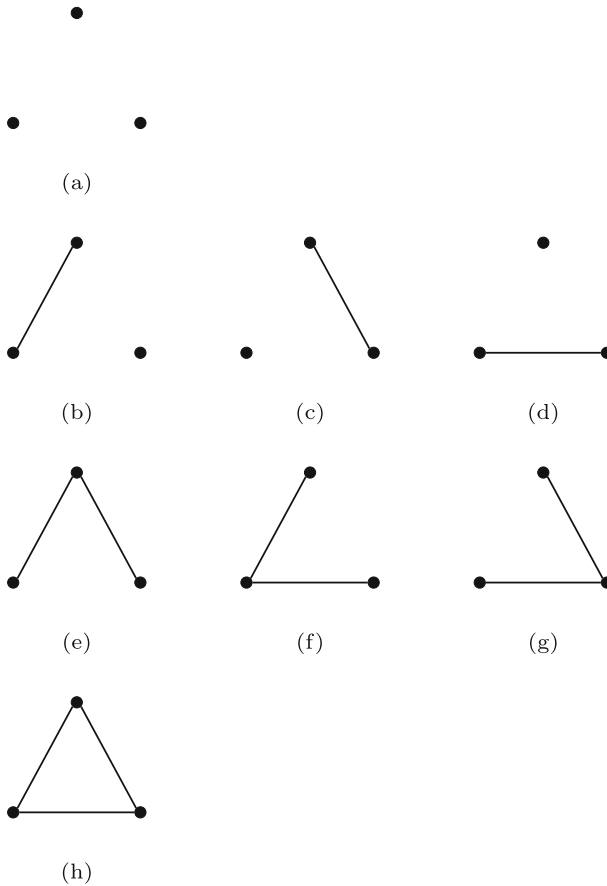
Fig. 3 Graphs with three vertices. It is easy to see that, unless the graph is labelled, in each row, all graphs are equivalent to the first one.

effect of permutations on the number of elements in a set after identifying equivalent elements. The cycle index is usually introduced in a very abstract form which makes it applicable to a wide range of applications but makes it difficult for those unfamiliar with the general theory to understand how it is applied in a particular situation. For our purpose of understanding the specific example of enumerating graphs we hope that the reader will find it simpler to consider the concrete example of a graph with three vertices to understand the principle of the construction of the cycle index. A general presentation of the theory can be found in Pólya (1937); Harary and Palmer (1973).

The cycle index represents each permutation that has been written in the disjoint cycle representation via a multivariate monomial $t_1^{\alpha_1} t_2^{\alpha_2} \ldots t_n^{\alpha_n}$. Here, each variable t_i stands for a cycle of length i and the exponent α_i accounts for how many times a cycle of length i occurs in a given permutation. This means that, for example, the permutation $(1)(2)(3)$ i.e. the identity is represented as t_1^3, for $(1)(23)$ we obtain $t_1 t_2$ and for (132) we have t_3^1.
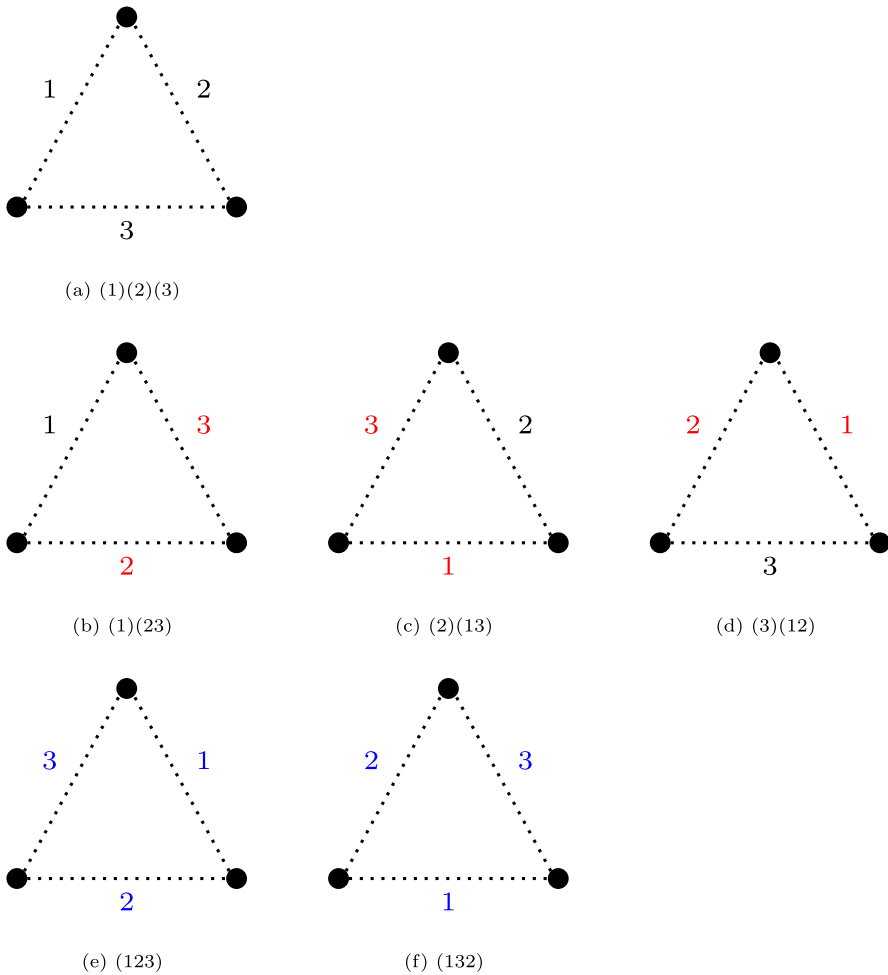
Fig. 4 Representation of the six different permutations of the graph with three vertices.

The benefit of introducing the variables t_i is that they allow us to account for the effect of a cycle of length i. Consider, for example, the permutation $(1)(23)$, see Fig. 4b. Because edges 2 or 3 are swapped, the resulting graph can only be equivalent if both edges are either present or absent i.e. for a cycle of length 2 we need to either draw none of the edges in the circle or both. This can be represented by the polynomial $1 + t^2$ where t^2 represents drawing two edges. Because edge 1 is not moved we can either include this edge in the graph or not which is represented, as above, as the polynomial $1 + t$. In general, to see the effect of a cycle of length i we replace the variable t_i with $1 + t^i$.

To account for multiple permutations with a particular combination of cycles—these permutations are said to have the same type—we multiply each monomial with the number of permutations of the type represented by this monomial.

The cycle index of the line group $\mathfrak{S}_3^{(2)}$ of graphs with $n_V = 3$ vertices is

$$Z(\mathfrak{S}_3^{(2)}; t_1, t_2, t_3) = \frac{1}{6}\left(t_1^3 + 3t_1t_2 + 2t_3\right) \tag{7}$$

where t_1^3 accounts for the identity, $3t_1t_2$ stands for the 3 permutations that swap two edges while not moving the remaining one and $2t_3$ represents the two permutations that move all three edges, see Fig. 4. The polynomial is scaled by the number of permutations in the symmetry group which results in the factor $\frac{1}{6}$.

According to Pólya's enumeration theorem, by evaluating the cycle index $Z(\mathfrak{S}_3^{(2)}, 1 + t, 1 + t^2, 1 + t^3)$ we can find a polynomial that represents the number of graphs with 3 vertices for different numbers of edges:

$$Z(1 + t, 1 + t^2, 1 + t^3) = \frac{1}{6}\left[(1 + t)^3 + 3 \cdot (1 + t)(1 + t^2) + 2 \cdot (1 + t^3)\right] \tag{8}$$
$$= 1 + t + t^2 + t^3. \tag{9}$$

This result indicates that among graphs with three vertices we can find one unlabelled graph each with zero, 1, 2 or 3 edges. This is consistent with Fig. 3.

Based on this example, we can conclude that Pólya enumeration relies on finding an expression of the cycle index for the symmetry group for a particular class of objects of interest. This is not an easy task and leads to a quite complicated closed-form formula in the general case. Because the main aim of this section is to explain the underlying idea of the enumeration of aggregated Markov models rather than explaining the calculation of the line group $\mathfrak{S}_n^{(2)}$ in full detail we refer the reader to chapter 4.1 in Harary and Palmer (1973). The number of graphs for a given number of vertices n_V, calculated in this way can be found in Table 1.

2.3 Graphs with coloured vertices and rooted graphs

Enumerating aggregated Markov models comes with the additional difficulty that the vertices of the graph can have two different "colours", say red and green, as in Fig. 3. An elegant solution for enumerating graphs with two colours is to consider rooted graphs, see Figure 5.

"Colour" is represented in a rooted graph by considering if a designated root node is adjacent to a vertex or not—in Fig. 5, a vertex which is adjacent to the root is coloured white, if it is not adjacent to the root it is coloured black. Representing the colour of a vertex as part of the structure of the graph is much simpler than attempting to investigate the different colourings of graphs under their respective symmetry groups. The calculation of the cycle index for rooted graphs is again described in Harary and Palmer (1973, chapter 4.4), results for the number of rooted graphs for a given number of vertices n_V are found in Table 1.
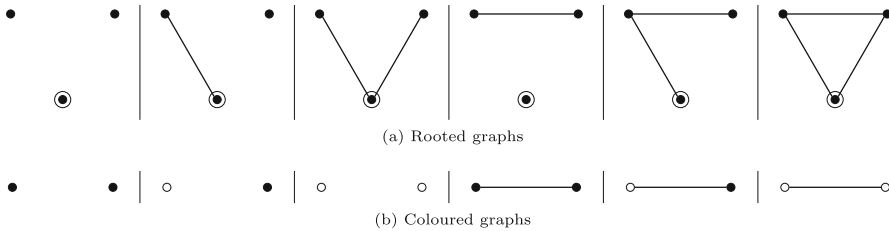
(a) Rooted graphs

(b) Coloured graphs

Fig. 5 Rooted graphs with 3 vertices and the corresponding coloured graphs with 2 vertices. Vertices that are adjacent to the root are represented as white in the corresponding coloured graph, vertices that are not adjacent are black.

2.4 Connected rooted graphs... and The End

In our attempt to enumerate the number of aggregated Markov models there is one difficulty that remains. Instead of all graphs whose vertices can have two colours we are, in fact, only interested in connected graphs. There is a general method for determining the number of connected graphs from the number of graphs with a given property. For this, we consider the formal power series (also known as the generating series)

$$g(t) = \sum_{k=1}^{\infty} g_k t^k \tag{10}$$

where g_p is the number of graphs with a certain property, for example, the number of arbitrary graphs or the number of rooted graphs with k vertices—note that in contrast to the examples for enumeration of graphs and rooted graphs considered above we are not enumerating graphs by the number of edges.

If we define, analogously to (10), the generating series $c(t)$ of connected graphs or rooted graphs, $g(t)$ and $c(t)$ are related by *Riddell's formula*[3] (Riddell 1951; Harary and Palmer 1973):

$$1 + g(t) = \exp\left(\sum_{k=1}^{\infty} \frac{1}{k} c(t^k)\right). \tag{11}$$

This relationship between graphs and connected graphs might look rather mysterious but it is based on the simple fact that for any graph we can determine the number of connected components. Thus, the number of graphs can be reconstructed by drawing connected graphs that will then become the connected components of a regular graph. The additional term $+1$ in (11) stands for the "empty" graph with no vertices. The relevant symmetry group for graphs consisting of n connected components is $\mathfrak{S}_n$ so

---

[3] In terms of integer sequences the relationship (11) is also known as an Euler transform.

that we obtain the cycle index

$$\sum_{k=1}^{\infty} Z(\mathfrak{S}_n; c(t)) =: Z(S_\infty, c(t)).$$
(12)

It can be shown that as a formal power series,

$$Z(\mathfrak{S}_\infty; c(t)) = \exp\left(\sum_{k=1}^{\infty} \frac{1}{k} c(t^k)\right).$$
(13)

By taking advantage of the arithmetic of formal power series—although this involves some tedious calculations—it is possible to use (11) for calculating the generating series $c(t)$ for connected graphs from the generating series $g(t)$ for arbitrary graphs. This process is also known as an inverse Euler transform of (11).

One possible solution is to set

$$\sum_{k=1}^{\infty} a_k t^k = \log(1 + g(t))$$
(14)

and calculate the coefficients a_k by coefficient matching with $\log(1 + g(t))$ as a power series. This yields the recursion formula

$$a_k = g_k - \frac{1}{k} \sum_{i=1}^{k-1} i \cdot a_i g_{k-i}.$$
(15)

Matching coefficients of $\sum_{k=1}^{\infty} a_k t^k$ with $\sum_{k=1}^{\infty} \frac{1}{k} \cdot c(t^k)$ leads to the relationship

$$a_k = \frac{1}{k} \sum_{d|k} d c_d.$$
(16)

Finally, the coefficients c_k of the generating series for connected graphs can be calculated from a_k by *Möbius inversion*:

$$c_k = \sum_{d|k} \frac{\mu(d)}{d} a_{p/d}$$
(17)

where $d|k$ stands for all divisors d of k and the Möbius function is defined as

$$\mu(k) = \begin{cases} 1 & \text{if } n = 1, \\ (-1)^k & \text{if } n \text{ is a product of } k \text{ distinct primes,} \\ 0 & \text{if } n \text{ is divisible by a square.} \end{cases}$$
(18)

Using the formulae (15) and (17) it is straightforward to calculate the number of connected graphs as well as the number of rooted graphs, see Table 1.

The number of connected rooted graphs with $n_V + 1$ vertices (including the root node) or, analogously, graphs with n_V vertices which have one of two different colours, also contains graphs that have only one of the two colours. Those graphs are examples for degenerate aggregated Markov models where only one of the two aggregates is present. Fortunately, it is not difficult to exclude these graphs—for every connected graph there are only two graphs that have only one colour—one in each colour. Thus, the number of (non-degenerate) aggregated Markov models M_k with n_V vertices is obtained from the number of coloured graphs CR_k by subtracting twice the number of connected graphs $2c_k$:

$$M_k = CR_k - 2 \cdot c_k. \tag{19}$$

3 Non-identifiability

One aspect of aggregated Markov models is that non-identifiability is a common phenomenon. Non-identifiability can be illustrated by the hypothetical situation that we know exactly the structure of the underlying model that generates the process that we observe. If the model is non-identifiable, it can generate identical behaviour when choosing different parameter sets. The reason why such a model is called non-identifiable can be explained by the somewhat counter-intuitive consequence that even if an infinite amount of data which is not perturbed by noise were available, the parameters of the model nevertheless could not be uniquely determined by fitting the model to these data.

3.1 Upper bound for the number of parameters in aggregated Markov models

The main result in this regard goes back to Fredkin et al. (1985); Fredkin and Rice (1986) who observed that the dynamics of aggregated Markov models can be completely represented by the bivariate distributions f_{OC} and f_{CO} of the length of an open time t_O followed by a closed time t_C and vice versa :

$$f_{OC}(t_O, t_C) = \sum_{i=1}^{n_O} \sum_{j=1}^{n_C} \alpha_{OC}^{ij} \exp\left(-\lambda_O^i t_O - \lambda_C^j t_C\right) \tag{20}$$

$$= \sum_{i=1}^{n_O} \sum_{j=1}^{n_C} \rho_{OC}^{ij} \lambda_O^i \lambda_C^j \exp\left(-\lambda_O^i t_O - \lambda_C^j t_C\right), \tag{21}$$

Table 1 Enumeration of graphs, rooted graphs, connected rooted graphs and aggregated Markov models obtained by Pólya enumeration as explained in Section 2. Note that for rooted and connected rooted graphs we have not counted the root node i.e. any rooted graphs with n_V vertices has $n_V + 1$ vertices including the root.

n_V	Graphs	Connected graphs	Rooted graphs	Connected rooted graphs	Aggregated Markov models
1	1	1	2	2	0
2	2	1	6	3	1
3	4	2	20	10	6
4	11	6	90	50	38
5	34	21	544	354	312
6	156	112	5096	3883	3659
7	1044	853	79264	67994	66288
8	12346	11117	2208612	2038236	2016002
9	274668	261080	113743760	1091141344	108619184
10	12005168	11716571	10926227136	10693855251	10670422109

$$f_{CO}(t_C, t_O) = \sum_{j=1}^{n_C} \sum_{i=1}^{n_O} \alpha_{CO}^{ji} \exp\left(-\lambda_C^j t_C - \lambda_O^i t_O\right), \tag{22}$$

$$= \sum_{j=1}^{n_C} \sum_{i=1}^{n_O} \rho_{CO}^{ji} \lambda_C^j \lambda_O^i \exp\left(-\lambda_C^j t_C - \lambda_O^i t_O\right). \tag{23}$$

Note that here, the parameters λ_O^i and λ_C^j are the negatives of eigenvalues of sub-matrices of the infinitesimal generator Q of the aggregated Markov model.

The bivariate distributions (20), (22) can also be represented as bilinear forms. By defining the matrices

$$\boldsymbol{\alpha}_{OC} = \left(\alpha_{OC}^{ij}\right) \tag{24}$$

$$\boldsymbol{\alpha}_{CO} = \left(\alpha_{CO}^{ji}\right) \tag{25}$$

we obtain

$$f_{OC}(t_O, t_C) = \left(\exp(-\lambda_O^1 t_O), \exp(-\lambda_O^2 t_O), \ldots, \exp(-\lambda_O^{n_O} t_O)\right) \boldsymbol{\alpha}_{OC} \begin{pmatrix} \exp(-\lambda_C^1 t_C) \\ \exp(-\lambda_C^2 t_C) \\ \vdots \\ \exp(-\lambda_C^{n_C} t_C) \end{pmatrix} \tag{26}$$

$$f_{CO}(t_C, t_O) = \left(\exp(-\lambda_C^1 t_C), \exp(-\lambda_C^2 t_C), \ldots, \exp(-\lambda_C^{n_C} t_C)\right) \boldsymbol{\alpha}_{CO} \begin{pmatrix} \exp(-\lambda_O^1 t_O) \\ \exp(-\lambda_O^2 t_O) \\ \vdots \\ \exp(-\lambda_O^{n_O} t_O) \end{pmatrix} \tag{27}$$

Using the result from (Fredkin et al. 1985; Fredkin and Rice 1986) that all information on the dynamics of an aggregated Markov model is contained in the bivariate distributions f_{OC} and f_{CO} (Theorem 4.1 in Fredkin et al. (1985), and Theorem A in Fredkin and Rice (1986))[4], we can find the maximal number of free parameters of an aggregated Markov by answering the simpler question how many parameters the distributions f_{OC} and f_{CO} depend on. The numbers of free parameters in the univariate

---

[4] More formally, the statement that "all information on the dynamics of an aggregated Markov model is contained in the bivariate distributions f_{OC} and f_{CO}" means that the parameters of higher-order distributions such as f_{OCO} or f_{COC} are uniquely determined by the bivariate distributions f_{OC} and f_{CO}. See Fredkin et al. (1985); Fredkin and Rice (1986).

distributions f_O and f_C are contained in this number because these distributions can be obtained by marginalising the bivariate distributions, for example,

$$f_O(t_O) = \int_0^\infty f_{OC}(t_O, t_C) dt_C = \sum_{j=1}^{n_C} \sum_{i=1}^{n_O} \frac{\alpha_{OC}^{ij}}{\lambda_C^j} \exp\left(-\lambda_O^i t_O\right), \qquad (28)$$

$$= \sum_{i=1}^{n_O} \underbrace{\left(\sum_{j=1}^{n_C} \frac{\alpha_{OC}^{ij}}{\lambda_C^j}\right)}_{\alpha_O^i} \exp\left(-\lambda_O^i t_O\right), \qquad (29)$$

To determine the number of parameters contained in the distributions f_{OC} and f_{CO}[5] we follow the derivation given in Fredkin et al. (1985, Corollary 4.1).

To find the total number of free parameters contained in f_{OC} and f_{CO} we consider (22) or (26) and observe that we have to account for the n_O rates λ_O^i and the n_C rates λ_C^j and add them to the number of parameters contained in α_{OC}^{ij} and α_{CO}^{ji}. Considering that the α_{OC}^{ij} and α_{CO}^{ji} can be interpreted as tables with $n_O \cdot n_C$ parameters each, the number of parameters that both α_{OC}^{ij} and α_{CO}^{ji} depend on appears to be $2n_O n_C$ so that the total number of parameters would be $2n_O n_C + n_O + n_C$. But there are a few constraints that reduce this number.

First of all, considering only one of the distributions, say f_{OC}, we observe that the number of parameters is reduced by one—because f_{OC} is a probability distribution, the ρ_{OC}^{ij}, see (21), have to sum up to one. This yields $n_O n_C - 1$ free parameters.

Second, there are constraints that arise from the coupling of α_{OC}^{ij} and α_{CO}^{ji} introduced by the fact that f_O and f_C can both be obtained from the bivariate distributions f_{OC} and f_{CO} via marginalisation. Calculating f_O by marginalising f_{OC} as shown in (28) is just one of two possibilities—f_O can also be calculated analogously to (28) from the distribution f_{CO}. Whilst marginalising f_{OC} yields coefficients $\alpha_O^i = \sum_{j=1}^{n_C} \frac{\alpha_{OC}^{ij}}{\lambda_C^j}$, marginalising f_{CO} leads to coefficients α_O^i that depend on the α_{CO}^{ji} instead. Because calculating the coefficients α_O^i from f_{CO} instead of f_{OC} must not change their value, we obtain the constraints

$$\sum_{j=1}^{n_C} \frac{\alpha_{CO}^{ji}}{\lambda_C^j} = \sum_{j=1}^{n_C} \frac{\alpha_{OC}^{ij}}{\lambda_C^j}, \quad i = 1, \dots, n_O \qquad (30)$$

---

[5] Note that by considering the distributions f_{OC} and f_{CO}, the upper bound for parameters derived by Fredkin et al. (1985); Fredkin and Rice (1986) is only valid for processes that are at equilibrium. Recordings from single ion channels are usually started after the channels had sufficient time to adjust to the experimental conditions such as, for example, ligand concentrations. For this reason, the assumption that the ion channel dynamics $\mathcal{D}$ has reached equilibrium is justified. A theory for the non-identifiability of aggregated Markov models that have not reached the stationary distribution has been developed by Ito et al. (1992) for discrete-time aggregated Markov models and was then transferred to the continuous case by Rydén (1996).

and analogously, by considering the calculation of f_C via marginalisation of f_{OC} and f_{CO}, respectively, further constraints

$$\sum_{i=1}^{n_O} \frac{\alpha_{CO}^{ji}}{\lambda_O^i} = \sum_{i=1}^{n_O} \frac{\alpha_{OC}^{ij}}{\lambda_O^i}, \quad j = 1, \ldots, n_C \tag{31}$$

on the α_{CO}^{ji} are obtained. Interpreting α_{CO}^{ji} as a $n_C \times n_O$ matrix, these constraints allow us to calculate one element in each column from the equations in (30) and, similarly, using (31), one element in each row of $\left(\alpha_{CO}^{ji}\right)$ from the α_{OC}^{ij} and other entries in the same row or column. This means that the $n_C \times n_O$ matrix $\left(\alpha_{CO}^{ji}\right)$ effectively has only $(n_O - 1)(n_C - 1)$ components. Thus, in total counting the number of independent parameters contained in the coefficients α_{OC}^{ij} and α_{CO}^{ji} we conclude that there are

$$n_O n_C - 1 + (n_O - 1)(n_C - 1) = 2n_O n_C - n_O - n_C \tag{32}$$

Now, taking into account that there are n_O rate constants λ_O^i and n_C rate constants λ_C^j we find that in total there are at most $2n_O n_C$ independent parameters in the distributions f_{OC} and f_{CO}.

We note that a refined upper bound for the maximum number of rates of an aggregated Markov model has been derived in Fredkin and Rice (1986). Apart from the numbers of open and closed, Fredkin and Rice (1986) also considered the rank of the transmission matrices Q_{CO} and Q_{OC}. For more details we refer the reader to Lemma A in Fredkin and Rice (1986) where this result is presented.

3.2 Alternative derivation of the upper bound $2n_O n_C$

We would like to derive the upper bound $2n_O n_C$ for the number of rate constants of an aggregated Markov model more directly, as presented previously in similar form in Kienker (1989). For this purpose it is useful to write the infinitesimal generator Q of an aggregated Markov in the form

$$\mathbf{Q} = \left(\begin{array}{c|c} \mathbf{Q}_{CC} & \mathbf{Q}_{CO} \\ \hline \mathbf{Q}_{OC} & \mathbf{Q}_{OO} \end{array} \right) \tag{33}$$

Although the matrix $\mathbf{Q}$ has $(n_O + n_C)^2$ components, for the diagonal elements q_{ii} we have $q_{ii} = -\sum_{j \neq i} q_{ij}$. Thus, at most $(n_O + n_C)(n_O + n_C - 1)$ components of $\mathbf{Q}$ can be freely chosen—this coincides with the number of directed edges in a complete graph with $n_V = n_O + n_C$ vertices and therefore the maximal number of rates.

But if the blocks $\mathbf{Q}_{CC}$ and $\mathbf{Q}_{OO}$ are diagonalisable it is possible to reparametrise the model $\mathbf{Q}$ so that all components within $\mathbf{Q}_{CC}$ and $\mathbf{Q}_{OO}$ except for the diagonal vanish—without changing the dynamics $\mathcal{D}$! Thus, we consider block-wise similarity

transformations $\mathbf{S}$ introduced by Kienker (1989)

$$\mathbf{S} = \left(\begin{array}{c|c} \mathbf{S}_{CC} & \mathbf{0}_{CO} \\ \hline \mathbf{0}_{OC} & \mathbf{S}_{OO} \end{array}\right) \qquad (34)$$

where $\mathbf{S}_{CC} \in \mathbb{R}^{n_C \times n_C}$ and $\mathbf{S}_{CC} \in \mathbb{R}^{n_O \times n_O}$ are invertible matrices and $\mathbf{0}_{CO} \in \mathbb{R}^{n_C \times n_O}$, $\mathbf{0}_{OC} \in \mathbb{R}^{n_O \times n_C}$ are matrices of zeroes. It is easy to see that

$$\mathbf{S}^{-1} = \left(\begin{array}{c|c} \mathbf{S}_{CC}^{-1} & \mathbf{0}_{CO} \\ \hline \mathbf{0}_{OC} & \mathbf{S}_{OO.}^{-1} \end{array}\right) \qquad (35)$$

If we consider models $\mathbf{Q}' = \mathbf{S}^{-1}\mathbf{Q}\mathbf{S}$, it is well-known that the eigenvalues $-\lambda_C^1, \ldots, -\lambda_C^{n_C}$ and $-\lambda_O^1, \ldots, -\lambda_O^{n_O}$ are invariants but Kienker (1989) demonstrates in his Lemmata 1 and 2 that even the probability distributions f_C, f_O, f_{CO} and f_{OC} are preserved under block-wise similarity transformations. This means that the dynamics $\mathcal{D}$ of a model $\mathbf{Q}' = \mathbf{S}^{-1}\mathbf{Q}\mathbf{S}$ is indistinguishable from the model $\mathbf{Q}$. For this reason, the models $\mathbf{Q}'$ and $\mathbf{Q}$ are called *equivalent*.

The upper bound $2n_O n_C$ can now be easily derived if the block matrices $\mathbf{Q}_{CC}$ and $\mathbf{Q}_{OO}$ are diagonalisable. This is true for models that fulfil the *detailed balance conditions* (57) which will be discussed in more detail below. Because the detailed balance conditions are related to the thermodynamic principle also known as the Second Law of Thermodynamics that entropy can never decrease in a closed system (when interpreting a Markov model as a representation of a chemical system), detailed balance is often assumed for Markov models of ion channels.

For diagonalisable $\mathbf{Q}_{CC}$ and $\mathbf{Q}_{OO}$, we can find a matrix $\mathbf{T} = \left(\begin{array}{c|c} \mathbf{T}_{CC} & \mathbf{0}_{CO} \\ \hline \mathbf{0}_{OC} & \mathbf{T}_{OO} \end{array}\right)$ that brings the blocks $\mathbf{Q}_{CC}$ and $\mathbf{Q}_{OO}$ to diagonal form:

$$\mathbf{Q}' = \mathbf{T}^{-1}\mathbf{Q}\mathbf{T} = \left(\begin{array}{c|c} \mathbf{T}_{CC}^{-1}\mathbf{Q}_{CC}\mathbf{T}_{CC} & \mathbf{T}_{CC}^{-1}\mathbf{Q}_{CO}\mathbf{T}_{OO} \\ \hline \mathbf{T}_{OO}^{-1}\mathbf{Q}_{OC}\mathbf{T}_{CC} & \mathbf{T}_{OO}^{-1}\mathbf{Q}_{OO}\mathbf{T}_{OO} \end{array}\right) \qquad (36)$$

$$= \left(\begin{array}{cccc|cccc} -\lambda_C^1 & 0 & \ldots & 0 & & & & \\ 0 & -\lambda_C^2 & \ddots & \vdots & & \overbrace{\mathbf{T}_{CC}^{-1}\mathbf{Q}_{CO}\mathbf{T}_{OO}}^{n_O}\} n_C & & \\ \vdots & \ddots & \ddots & 0 & & & & \\ 0 & \ldots & 0 & -\lambda_C^{n_C} & & & & \\ \hline & & & & -\lambda_O^1 & 0 & \ldots & 0 \\ & & & & 0 & -\lambda_O^2 & \ddots & \vdots \\ & n_O\{\underbrace{\mathbf{T}_{OO}^{-1}\mathbf{Q}_{OC}\mathbf{T}_{CC}}_{n_C} & & & \vdots & \ddots & \ddots & 0 \\ & & & & 0 & \ldots & 0 & -\lambda_O^{n_O} \end{array}\right) \qquad (37)$$

From (37) it is now clear that the transformed matrix can at most depend on $2n_O n_C$ free parameters—the diagonal elements q'_{ii} can again be disregarded because they are determined by the off-diagonal elements and the matrices $\mathbf{Q}'_{CO}$ and $\mathbf{Q}'_{OC}$ have $n_O n_C$ parameters each.

This calculation also shows that it is possible to find a reparametrisation of any fully connected aggregated Markov model to an aggregated Markov model with $2n_O n_C$ rate constants (which therefore fulfils the necessary condition for identifiability). However, as we will see in Section 3.4.1 where this transformation is carried out explicitly for the fully connected three-state model, this does not always yield a feasible model—as we will observe, there are parameter sets for which some of the rates in the reparametrised model are negative.

The matrix (37) defines a model structure where all transition rates from open to other open states or between closed states vanish—all transitions occur between open and closed states. This structure has been proposed as a *canonical from* for models with a given number of n_O open and n_C closed states. Canonical forms provide models that are parameter-identifiable and can be used as representatives for equivalence classes of models. The particular form (37) has been studied by Bauer et al. (1987); Kienker (1989) and is referred to as *Bauer-Kienker uncoupled (BKU) form* in Bruno et al. (2005). For a brief discussion of canonical forms see the Discussion (Section 4).

3.3 Interpretation of sojourn time distributions

The reduction of aggregated Markov models to the bivariate distributions f_{OC} and f_{CO} (Fredkin et al. 1985; Fredkin and Rice 1986) leads to an alternative interpretation of the dynamics $\mathcal{D}$. This leads to a more abstract view compared to the illustrative transitions between open and closed states which are assigned additional biophysical significance by associating them with different conformational states of the channel protein. Figure 6 illustrates that the distributions f_C, f_O, f_{OC} and f_{CO} can be interpreted as two-stage processes where a finite distribution is used for determining which distributions are used for generating either sojourn times or pairs of subsequent sojourn times. Figure 6a illustrates how the coefficients $\boldsymbol{\rho}_O$ define a finite distribution that stochastically selects if an open time is generated from a "slow" or "fast" exponential state. As shown in Figure 6b this is extended to the distribution f_{OC} which generates an open time followed by a closed time. After an open and a closed exponential state have been chosen by the finite distribution defined by the components ρ_{OC}^{ij} of the matrix $\boldsymbol{\rho}_{OC}$, a pair (t_O, t_C) of subsequent open and closed times is generated.

3.4 *Example:* The fully connected three-state model

In order to illustrate the consequences of this abstract result by Fredkin et al. (1985); Fredkin and Rice (1986) with a concrete example, let us consider the simplest case of a non-identifiable model, the fully connected three-state model. We follow and expand
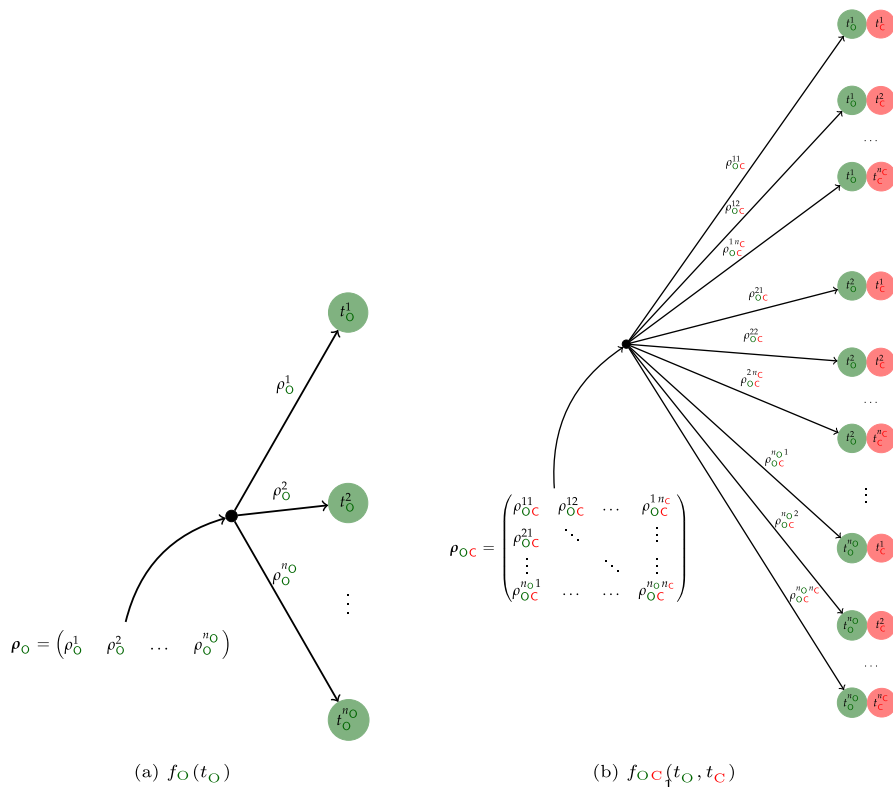
(a) $f_O(t_O)$
(b) $f_{OC}(t_O, t_C)$

Fig. 6 Graphical illustration of the sojourn time distribution $f_O(t_O)$ and the bivariate distribution $f_{OC}(t_O, t_C)$ as mixtures of exponential distributions—the distributions $f_C(t_O)$ and $f_{CO}(t_C, t_O)$ are analogous. It shows that sojourn times t_O are generated in a two-stage process. First, from the finite distribution defined by ρ_O, an exponential distribution t_O^i is chosen which then generates an open time t_O, see (a). Similarly, the matrix ρ_{OC} defines a finite distribution over pairs of exponential distributions. After choosing a pair (t_O^i, t_C^j), $i = 1, \ldots, n_O$, $j = 1, \ldots, n_C$, it generates an open time t_O and a subsequent closed time t_C, see (b).

the presentation from Kienker (1989):

$$Q = \begin{pmatrix} -q_{12} - q_{13} & q_{12} & q_{13} \\ q_{21} & -q_{21} - q_{23} & q_{23} \\ q_{31} & q_{32} & -q_{32} - q_{31} \end{pmatrix} \tag{38}$$

The matrix Q in (38) is partitioned in the closed compartment $C = \{C_1, C_2\}$ and the open compartment $O = \{O_3\}$. It is helpful to summarise the parameters of the model via the sojourn time distributions $f_O(t)$ and $f_C(t)$:

$$f_C(t_C) = \rho \lambda_C^1 \exp(-\lambda_C^1 t_C) + (1 - \rho) \lambda_C^2 \exp(-\lambda_C^2 t_C), \tag{39}$$

$$f_O(t_O) = \lambda_O^1 \exp(-\lambda_O^1 t_O) \tag{40}$$

The two distributions f_C and f_O together depend on four independent parameters—the weight ρ of the first component in the mix of two exponential distributions that f_C consists of as well as the rates λ_C^1, λ_C^2 and λ_O^1 which are eigenvalues of submatrices of the matrix Q.

Because eigenvalues depend in an increasingly complex way on the components of a matrix as the dimension increases, it is advantageous to alternatively consider

$$T_C := \operatorname{Tr} Q_{CC} = -q_{12} - q_{13} - q_{21} - q_{23} = -\lambda_C^1 - \lambda_C^2, \tag{41}$$

$$D_C := \det Q_{CC} = q_{12}q_{23} + q_{13}q_{21} + q_{13}q_{23} = \lambda_C^1 \cdot \lambda_C^2, \tag{42}$$

$$S := Q_{OC} Q_{CO} = q_{13}q_{31} + q_{23}q_{32}, \tag{43}$$

$$T_O := \operatorname{Tr} Q_O = -q_{31} - q_{32} = -\lambda_O^1. \tag{44}$$

when evaluating transformations of the generator Q. In order to investigate non-identifiability, we are interested in reparametrisations of the matrix Q that alter the rate constants q_{ij} but leave the parameters of the sojourn time distributions invariant.

For the three-state model, the rates of the closed-time distribution $f_C(t_C)$ are obtained as solutions of the characteristic polynomial of the matrix Q_{CC}

$$\lambda^2 - T_C \lambda + D_C = 0 \tag{45}$$

The weight ρ can be found by elementary but relatively tedious calculations

$$\rho = \frac{S - \lambda_O^1 \lambda_C^2}{\lambda_O^1 \cdot \left(\lambda_C^1 - \lambda_C^2\right)} = \frac{\frac{S}{\lambda_O^1} - \lambda_C^2}{\lambda_C^1 - \lambda_C^2}. \tag{46}$$

Because, in order to leave the closed time distribution $f_C(t_C)$ unchanged, the parameter ρ needs to be preserved by a reparametrisation and the expression (46) shows that S must be an invariant when reparametrising the model because all other parameters on the right-hand side of (46) are invariants. It also shows that it is possible to parameterise the three-state model, so that $\rho < 0$. In this case, the closed-time distribution f_C is a signed mixture of exponential distributions, rather than an ordinary mixture distribution for which all coefficients must be positive.

We will see in the following Section 3.4.1 that for $\rho > 0$ where f_C is a mixture of exponential distributions, the fully connected three-state model can be transformed to a reduced model with fewer rate constants, decreasing the original 6 parameters to a model with 4 parameters. In contrast, this will not be possible if f_C is a signed mixture of exponential distributions.

3.4.1 Transformation of the general three-state model to the model COC

We will attempt to reparametrise the model Q to obtain a model $\tilde{Q}$ with the same sojourn time distributions f_C and f_O. The model COC is a special case of the three-state model where both closed states C_1 and C_2 are adjacent to the open state O_3 but direct transitions between the closed states are not possible—$\tilde{q}_{12} = \tilde{q}_{21} = 0$. Because the matrix $\tilde{Q}_{CC} = \begin{pmatrix} -\tilde{q}_{13} & 0 \\ 0 & -\tilde{q}_{23} \end{pmatrix}$ is diagonal it follows that the rate constants $\tilde{q}_{13}$ and $\tilde{q}_{23}$ must coincide with the eigenvalues λ_C^1 and λ_C^2. For the remaining rate constants, in order to keep T_O and S invariant, we obtain linear equations in $\tilde{q}_{31}$ and $\tilde{q}_{32}$:

$$\tilde{q}_{31} + \tilde{q}_{32} = \lambda_O^1 \tag{47}$$

$$\tilde{q}_{13}\tilde{q}_{31} + \tilde{q}_{23}\tilde{q}_{32} = \lambda_C^1 \tilde{q}_{31} + \lambda_C^2 \tilde{q}_{32} = S \tag{48}$$

Interestingly, the solution

$$\tilde{q}_{31} = \frac{S - \lambda_O^1 \lambda_C^2}{\lambda_C^1 - \lambda_C^2} = \lambda_O^1 \frac{\frac{S}{\lambda_O^1} - \lambda_C^2}{\lambda_C^1 - \lambda_C^2} = \lambda_O^1 \cdot \rho \tag{49}$$

so that the model COC can be easily obtained from the distributions f_O and f_C by assigning the parameters ρ, λ_C^1, λ_C^2 and λ_O^1 to the appropriate rate constants of the model COC (this is, of course, the specific example of the transformation used in Section 3.2 to derive the upper bound $2n_O n_C$ for the maximum number of rates for the model with n_V vertices):

$$\tilde{Q} = \left(\begin{array}{cc|c} -\lambda_C^1 & 0 & \lambda_C^1 \\ 0 & -\lambda_C^2 & \lambda_C^2 \\ \hline \rho \cdot \lambda_O^1 & (1-\rho) \cdot \lambda_O^1 & -\lambda_O^1 \end{array} \right) \tag{50}$$

It seems that the non-identifiability problem—at least for the simple case of the full three-state model—has a very simple solution (deceptively simple as it turns out). Instead of considering the complete parameter space of the fully connected three-state model, the model is reduced to an equivalent COC model.

But this overlooks that this reduction is not always possible in a meaningful way—for some possible parameter choices of three-state model, a negative value for ρ is obtained. In this case, the rate constant $\tilde{q}_{31}$ is negative which contradicts the underlying assumption that the rate constants of a Markov generator are all non-negative.

3.4.2 Continuous reparametrisation of the fully connected three-state model

The fully connected model cannot only be transformed to the model COC but, in fact, to a continuous set of models parametrised by two of the rates. By considering that the quantities in (41)-(43) need to be invariant to preserve the sojourn time distributions f_O

and f_C these quantities can be taken as invariants that different parametrisations need to fulfil. We can, for example, choose q_{13} and q_{23} as free parameters and express the remaining rate constants as functions of q_{13} and q_{23} for given T_O, T_C, D_C and S.

From the relationship

$$q_{23}^2 + T_C q_{23} + D_C = q_{21}(q_{13} - q_{23}) \tag{51}$$

we can calculate:

$$q_{21} = \frac{q_{23}^2 + T_C q_{23} + D_C}{q_{13} - q_{23}} \tag{52}$$

This expression for q_{21} allows us—using the trace Tc in (41)— to derive

$$q_{12} = -\frac{q_{13}^2 + T_C q_{13} + D_C}{q_{13} - q_{23}} \tag{53}$$

Similarly, with S from (42) after replacing q_{32} using the trace T_O, equation (43), we can calculate:

$$q_{31} = \frac{S + T_O q_{23}}{q_{13} - q_{23}} \tag{54}$$

and finally

$$q_{32} = -T_O - \frac{S + T_O q_{23}}{q_{13} - q_{23}} = -\frac{S + T_O q_{13}}{q_{13} - q_{23}} \tag{55}$$

3.4.3 Transformation of the general three-state model to the model CCO

Setting $q_{13} = 0$ in the equations (52)-(55) we can calculate the rates of a model where q_{13} vanishes:

$$\tilde{Q} = \left(\begin{array}{cc|c} -\dfrac{\lambda_C^1 \lambda_C^2}{q_{23}} & \dfrac{\lambda_C^1 \lambda_C^2}{q_{23}} & 0 \\ -\dfrac{\left(q_{23} - \lambda_C^1\right)\left(q_{23} - \lambda_C^2\right)}{q_{23}} & -\dfrac{\left(\lambda_C^1 + \lambda_C^2\right)q_{23} + \lambda_C^1 \lambda_C^2}{q_{23}} & q_{23} \\ \hline \lambda_O^1 - \dfrac{S}{q_{23}} & \dfrac{S}{q_{23}} & -\lambda_O^1 \end{array} \right) \tag{56}$$

Interestingly, $q_{13} = 0$ does not imply $q_{31} = 0$. But q_{31} does vanish if we require the *detailed balance conditions*. By definition, the detailed balance conditions are

$$\pi_C^i q_{i3} = \pi_O^3 q_{3i}, \quad i = 1, 2 \tag{57}$$

$$\pi_O^3 q_{3i} = \pi_C^i q_{i3} \tag{58}$$

$$\pi_C^1 q_{12} = \pi_C^2 q_{21}. \tag{59}$$

If a vector $\boldsymbol{\pi}$ exists that fulfils these conditions it is a *stationary distribution* of the Markov model. It can be shown that these conditions are fulfilled provided that

$$q_{31} q_{12} q_{23} = q_{13} q_{32} q_{21}, \tag{60}$$

in general, the products of rates along all cycles that involve three or more states must be equal in either direction. With detailed balance it, of course, follows that if $q_{13} = 0$, $q_{31} = \lambda_O^1 - \frac{S}{q_{23}}$ must vanish as well—if $q_{13} = 0$ the left-hand side of (60) vanishes which implies that one of the rates on the left-hand side must be zero as well. Thus, $q_{23} = \frac{S}{\lambda_O^1}$ and we have

$$\tilde{Q} = \left(\begin{array}{cc|c} -\frac{\lambda_O^1 \lambda_C^1 \lambda_C^2}{S} & \frac{\lambda_O^1 \lambda_C^1 \lambda_C^2}{S} & 0 \\ -\frac{\lambda_O^1}{S}\left(\frac{S}{\lambda_O^1} - \lambda_C^1\right)\left(\frac{S}{\lambda_O^1} - \lambda_C^2\right) & \frac{-(\lambda_C^1 + \lambda_C^2)S + \lambda_O^1 \lambda_C^1 \lambda_C^2}{S} & \frac{S}{\lambda_O^1} \\ \hline 0 & \lambda_O^1 & -\lambda_O^1 \end{array} \right). \tag{61}$$

It is also possible to find a version of the model **OCC** for which $q_{12} = 0$ but $q_{21} \neq 0$ (this model does therefore not fulfil detailed balance). Substituting $q_{13} = \lambda_C^1$ in (52) and (54) and rewriting q_{31} and q_{32} using the expression for ρ from (46) yields

$$\tilde{Q} = \left(\begin{array}{cc|c} -\lambda_C^1 & 0 & \lambda_C^1 \\ \lambda_C^2 - q_{23} & -\lambda_C^2 & q_{23} \\ \hline \rho\left(1 - \frac{1-\rho}{\rho}\frac{\lambda_C^2 - q_{23}}{q_{23} - \lambda_C^1}\right) \cdot \lambda_O^1 & \left[1 - \rho\left(1 - \frac{1-\rho}{\rho}\frac{\lambda_C^2 - q_{23}}{q_{23} - \lambda_C^1}\right)\right] \cdot \lambda_O^1 & -\lambda_O^1 \end{array} \right) \tag{62}$$

For the resulting model in (62) it shows that for $q_{12} = 0$, an infinite set of equivalent models can be obtained by continuously varying $q_{23} \in \left(\lambda_C^1, \lambda_C^2\right]$.

3.4.4 Summary

Our analysis of the fully connected three-state model has illustrated the two aspects of identifiability introduced in the introduction— parameter identifiability and the identifiability of model structure.

Our analysis shows that, at least for the example of the fully connected three-state model, *parameter identifiability* and *identifiability of model structure* are closely linked as visualised in Figure 7. Both Figures 7a show parameter sets q_{ij} of the fully-connected three-state model that preserve the four invariants T_C, D_C, T_O and S, see (41)-(43). Because the three-state model is parametrised by six rates, we obtain an equivalence class that depends on two parameters such as, for example, the rates q_{13} and q_{23}, see Section 3.4.2. Both rates are constrained to finite intervals in order to ensure that all six rate constants of the three-state model are non-negative.

When considering this equivalence class of models, two fundamentally different cases can be distinguished—without loss of generality, we assume that $\lambda_C^1 < \lambda_C^2$:

(a) Reducible to acyclic model

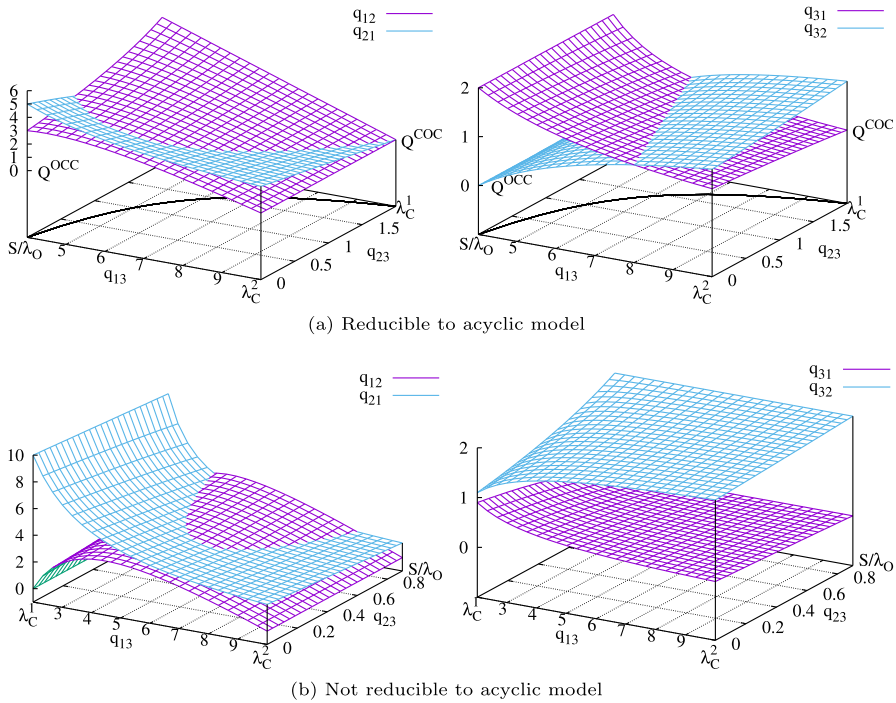(b) Not reducible to acyclic model

Fig. 7 Summary of the analysis of the complete three-state model. The rates q_{13} and q_{23} connecting the closed states C_1 and C_2 with the open state O_3. Without loss of generality we assume $q_{13} > q_{23}$ and $\lambda_C^1 < \lambda_C^2$. In (a), $\frac{S}{\lambda_O^1} \in \left[\lambda_C^1, \lambda_C^2\right]$. In this case, for all choices $q_{13} \in \left[\frac{S}{\lambda_O^1}, \lambda_C^2\right]$ and $q_{23} \in \left[0, \lambda_C^1\right]$, parametrisations can be found which produce the same stochastic dynamics. The parameter sets obtained for combinations of q_{13} and q_{23} along the curve on the base of the plot fulfil detailed balance, see (60). For $q_{13} = \frac{S}{\lambda_O^1}$, $q_{23} = 0$ we obtain the model OCC, for $q_{13} = \lambda_C^2$, $q_{23} = \lambda_C^1$ we obtain the model COC. The situation is fundamentally different in (b) where $\frac{S}{\lambda_O^1} < \lambda_C^1$. Here, the fully connected three-state model cannot be reduced to the acyclic model OCC or COC with non-negative rates. Also, in this case the closed time distribution f_C is not a mixture but a signed mixture of exponentials which generates a non-monotonous distribution. The set of equivalent models with non-negative rates in this case extends over the intervals $q_{13} \in \left[\lambda_C^1, \lambda_C^2\right]$ and $q_{23} \in \left[0, \frac{S}{\lambda_O^1}\right]$. The detailed balance condition (60) cannot be fulfilled for any of these models.

1. If $\frac{S}{\lambda_O^1} \in [\lambda_C^1, \lambda_C^2]$, the models COC and CCO are contained in the equivalence class. In this case, parameter identifiability can be resolved by selecting either COC or CCO as a representative of the equivalence class. In this way, non-identifiable models with six rates can be *reduced* to either of the two identifiable models COC or CCO with four rates. This case is visualised in Figure 7a.

2. If $\frac{S}{\lambda_O^1} \notin [\lambda_C^1, \lambda_C^2]$, it is not possible to reduce models in the equivalence class to either COC or CCO so that the rates are all non-negative. Thus, in this case, the parameter non-identifiability cannot be resolved because it is not possible to choose

any of the parameter-identifiable models COC or CCO as a representative. Also, in this case, the detailed balance conditions (57) cannot be fulfilled. Parameter sets of this type are visualised in Figure 7b.

By considering (46), we find that the condition $\frac{S}{\lambda_O^1} \in [\lambda_C^1, \lambda_C^2]$ is equivalent to $\rho > 0$. This means that models are reducible to an identifiable model if the closed time distribution f_C is a mixture of exponentials. In the opposite case $\frac{S}{\lambda_O^1} \notin [\lambda_C^1, \lambda_C^2]$ we find, in contrast, that the closed time distribution is a signed mixture of exponential distribution—here, the coefficients ρ and $1 - \rho$ of the closed time distribution f_C sum to one but either ρ or $1 - \rho$ is negative.

Because in this case, where the closed time distribution f_C is a non-monotonous signed mixture of exponentials, it is not possible to find a representative that is parameter-identifiable, this means that there are dynamics $\mathcal{D}$ which cannot be represented by an identifiable model which means that it is not possible to identify an unambiguous "mechanism" that can be represented using aggregated Markov models which generates this dynamics $\mathcal{D}$. To the best of our knowledge this phenomenon which deserves further attention has not been systematically investigated for aggregated Markov models with a larger number of states.

3.5 Model structure and biophysical mechanism[6]

We will now investigate the question if natural mechanistic models for the dependency of a ligand-gated ion channel on the ligand concentration c can help us decide which of the models COC or CCO might be preferable for a given data set. Although we have shown previously that both models are equivalent, they represent quite different mechanisms if we assume that the transitions between the model states are modulated by ligand binding sites. The model COC represents two *independent ligand binding* sites which can either facilitate or inhibit the transition to the open state. In contrast, CCO models *sequential binding*—a first ligand binding site increases the transition rate from the closed state C_1 to C_2 whereas a second binding site (which becomes accessible when the channel has transitioned to C_2) then activates the channel. To transform between the two models we can use (50) and (56) to directly relate the rates of the models COC and CCO:

$$q_{12}^{CCO} = \frac{q_{13}^{COC} q_{23}^{COC} \left(q_{31}^{COC} + q_{32}^{COC} \right)}{q_{13}^{COC} q_{31}^{COC} + q_{23}^{COC} q_{32}^{COC}} \tag{63}$$

$$q_{21}^{CCO} = \frac{\left(q_{13}^{COC} - q_{23}^{COC} \right)^2}{q_{13}^{COC} q_{31}^{COC} + q_{23}^{COC} q_{32}^{COC}} \frac{q_{31}^{COC} q_{32}^{COC}}{q_{31}^{COC} + q_{32}^{COC}} \tag{64}$$

---

[6] More than 10 years ago, Edmund Crampin and I had several passionate (but enjoyable) discussions about the "right" approach for modelling ion channels. Edmund suggested that I look at the relationship between different models for ligand binding and non-identifiability. This section is a first attempt to investigate the implications of non-identifiability on mechanistic models.

$$q_{23}^{\text{CCO}} = \frac{q_{13}^{\text{COC}} q_{31}^{\text{COC}} + q_{23}^{\text{COC}} q_{32}^{\text{COC}}}{q_{31}^{\text{COC}} + q_{32}^{\text{COC}}} \tag{65}$$

$$q_{32}^{\text{CCO}} = q_{31}^{\text{COC}} + q_{32}^{\text{COC}} \tag{66}$$

One aspect of (63)-(66) is that these expressions clearly show that an arbitrary model of the from COC can be transformed to a CCO model—if the rates q_{13}^{COC}, q_{23}^{COC}, q_{31}^{COC} and q_{32}^{COC} are positive, the rates q_{12}^{CCO}, q_{21}^{CCO}, q_{23}^{CCO} and q_{32}^{CCO} or q_{13}^{COC}, q_{23}^{COC}, q_{31}^{COC} and q_{32}^{COC} of the transformed model are positive as well.

But our primary interest is to investigate the effect of this transformation for different assumptions on the ligand dependencies of the model COC. For simplicity, we will assume that all dependencies are modelled via mass action. We will drop the superscripts for the rates of the models CCO and COC, instead we will use q_{13}, q_{23}, q_{31} and q_{32} when we refer to rates of the model COC and $\tilde{q}_{12}, \tilde{q}_{13}, \tilde{q}_{21}$ and $\tilde{q}_{31}$ when we refer to rates in the model CCO obtained via transformation of the model COC.

3.5.1 Two activating binding site

First, we assume that the channel has two activating binding sites. This implies that the rates q_{13} and q_{23} entering the open state are ligand-dependent and the rates q_{31} and q_{32} are constant i.e. independent from the ligand concentration c:

$$q_{13} = k_{13}c, q_{23} = k_{23}c, q_{31} = k_{31}, q_{32} = k_{32}. \tag{67}$$

Replacing (63)-(66) we observe that the resulting rate constants for the model CCO are:

$$\tilde{q}_{12} = \tilde{k}_{12}c, \tilde{q}_{21} = \tilde{k}_{21}c, \tilde{q}_{23} = \tilde{k}_{23}c, \tilde{q}_{32} = \tilde{k}_{32}. \tag{68}$$

with, as can simply be seen,

$$\tilde{k}_{12} = \frac{k_{13}k_{23}(k_{31} + k_{32})}{k_{13}k_{31} + k_{23}k_{32}} \tag{69}$$

$$\tilde{k}_{21} = \frac{(k_{13} - k_{23})^2}{k_{13}k_{31} + k_{23}k_{32}} \frac{k_{31}k_{32}}{k_{31} + k_{32}} \tag{70}$$

$$\tilde{k}_{23} = \frac{k_{13}k_{31} + k_{23}k_{32}}{k_{31} + k_{32}} \tag{71}$$

$$\tilde{k}_{32} = k_{31} + k_{32} \tag{72}$$

From a modelling point of view, the resulting CCO model is unusual. It appears that the activating binding sites that facilitate the transitions rate from the closed states C_1 and C_2 to the open state O_3 translate to activating binding sites that enable the transition from C_1 via C_2 to O_3. But although unbinding from binding sites would normally assumed to be ligand-independent, the transition q_{21} from C_2 to C_1 is again a mass action rate dependent on c. This implies that in order to reproduce the behaviour of the COC model, a ligand-dependent rate that inhibits the channel for large c by transitioning to the state C_1 seems to be required.

3.5.2 One activating binding site

Now, we assume that, of the two transitions to the open state, one is activated by ligand binding whereas the other transition is ligand-independent:

$$q_{13} = k_{13}c, \, q_{23} = k_{23}, \, q_{31} = k_{31}, \, q_{32} = k_{32}. \tag{73}$$

Replacing (63)-(66) we observe that the resulting rate constants for the model CCO are:

$$\tilde{q}_{12} = \tilde{F}_{12} \frac{c}{\tilde{H}_{12} + c}, \tag{74}$$

$$\tilde{q}_{21} = \frac{(k_{13}c - k_{23})^2}{k_{13}k_{31}c + k_{23}k_{32}} \frac{k_{31}k_{32}}{k_{31} + k_{32}} = \tilde{F}_{21} \frac{\left(c - \frac{k_{23}}{k_{13}}\right)^2}{\tilde{H}_{21} + c} \tag{75}$$

$$\tilde{q}_{23} = \frac{k_{13}k_{31}c + k_{23}k_{32}}{k_{31} + k_{32}} = \tilde{k}_{23}c + \tilde{K}_{23} \tag{76}$$

$$\tilde{q}_{32} = k_{31} + k_{32} \tag{77}$$

with

$$\tilde{F}_{12} = \frac{k_{23}(k_{31} + k_{32})}{k_{31}}, \, \tilde{H}_{12} = \frac{k_{23}k_{32}}{k_{13}k_{31}} \tag{78}$$

$$\tilde{F}_{21} = \frac{k_{13}k_{32}}{k_{31} + k_{32}}, \, \tilde{H}_{21} = \tilde{H}_{12} = \frac{k_{23}k_{32}}{k_{13}k_{31}} \tag{79}$$

$$\tilde{k}_{23} = \frac{k_{13}k_{31}}{k_{31} + k_{32}}, \, \tilde{K}_{23} = \frac{k_{23}k_{32}}{k_{31} + k_{32}} \tag{80}$$

For a COC model with one activating binding site and one ligand-independent, we find that $\tilde{q}_{12}$ has the form of a Michaelis-Menten term with maximum rate $\tilde{F}_{12}$ and half-saturation constant $\tilde{H}_{12}$. For $\tilde{q}_{21}$ we obtain another Hill function type term with a numerator of degree 2 and denominator of degree 1. This means that for large c, rate $\tilde{q}_{21}$ behaves like a mass action term, although, initially, it even decreases until vanishing at $\frac{k_{23}}{k_{13}}$. The rate $\tilde{q}_{23}$ is a mass action rate boosted with a constant influx $\tilde{K}_{23}$. Thus, for a COC model with one activating and one ligand-independent transition to the open state, a qualitatively different model is obtained. Rather than linearly increasing with

the ligand concentration c, the transition rate $\tilde{q}_{12}$ shows a saturating behaviour—it tends to the maximum rate $\tilde{F}_{12}$ for large c. The rate $\tilde{q}_{21}$ is again ligand-dependent with a more complicated dependency on the ligand concentration c which, however, behaves like a mass action term for large c. The transition $\tilde{q}_{23}$ is a mass action term, but with an additive ligand-independent constant $\tilde{K}_{23}$.

3.5.3 One activating and one inhibitory binding site

We now consider the case that one of the two binding site facilitates the transition from C_1 to the open state O_3 whereas the other one increases the rate to the closed state C_2 i.e. the channel has one activating and one inhibitory binding site

$$q_{13} = k_{13}c, \, q_{23} = k_{23}, \, q_{31} = k_{31}, \, q_{32} = k_{32}c. \tag{81}$$

Using (63)-(66), the rates of the model CCO are:

$$\tilde{q}_{12} = \frac{k_{13}k_{23}(k_{31} + k_{32}c)}{k_{13}k_{31} + k_{23}k_{32}} = \tilde{k}_{12}c + \tilde{K}_{12}, \tag{82}$$

$$\tilde{q}_{21} = \frac{(k_{13}c - k_{23})^2}{k_{13}k_{31} + k_{23}k_{32}} \frac{k_{31}k_{32}}{k_{31} + k_{32}c} = \tilde{F}_{21} \frac{\left(c - \frac{k_{23}}{k_{13}}\right)^2}{\tilde{H}_{21} + c} \tag{83}$$

$$\tilde{q}_{23} = \frac{k_{13}k_{31} + k_{23}k_{32}}{k_{31} + k_{32}c}c = \tilde{F}_{23} \frac{c}{\tilde{H}_{23} + c} \tag{84}$$

$$\tilde{q}_{32} = k_{31} + k_{32}c = \tilde{k}_{32}c + \tilde{K}_{32} \tag{85}$$

with

$$\tilde{k}_{12} = \frac{k_{12}k_{23}k_{32}}{k_{13}k_{31} + k_{23}k_{32}}, \, \tilde{K}_{12} = \frac{k_{12}k_{23}k_{31}}{k_{13}k_{31} + k_{23}k_{32}}, \tag{86}$$

$$\tilde{F}_{21} = \frac{k_{13}^2 k_{31}}{k_{13}k_{31} + k_{23}k_{32}}, \, \tilde{H}_{21} = \frac{k_{31}}{k_{32}} \tag{87}$$

$$\tilde{F}_{23} = \frac{k_{13}k_{31} + k_{23}k_{32}}{k_{32}}, \, \tilde{H}_{23} = \tilde{H}_{21} = \frac{k_{31}}{k_{32}}, \tag{88}$$

$$\tilde{k}_{32} = k_{32}, \, \tilde{K}_{32} = k_{31}. \tag{89}$$

For a model with one activating and one inhibitory binding site, we see similar terms as for the model with one activating and one ligand-independent transition that we considered in the previous section. Here, q_{12} and q_{32} are mass action terms with an additional ligand-independent offset. The transition to the open state, q_{23}, is again represented by a Michaelis-Menten term whereas the rate $\tilde{q}_{21}$ tends to a mass action rate for large c.

3.5.4 Summary

Our analysis of different mechanisms of ligand binding in the model COC has shown that by transformation to the model CCO, the dependency of some rates on the ligand concentration c might be changed from mass action kinetics to a Michaelis-Menten term, see Sections 3.5.2 and 3.5.3. In addition, even if all rates in the transformed model CCO are mass action terms, an additional ligand dependency might appear (here, in the transition q_{21} between the closed states C_2 and C_1, see Section 3.5.1) . It remains to be seen if these differences are sufficient to allow, in practice, to distinguish between independent binding sites (as represented in the model COC) and sequential binding (as in the model COC) by comparing fits of both model structures to experimental data.

4 Discussion

We have given an overview of the identifiability theory of aggregated Markov models. Aggregated Markov models appear naturally in the modelling of ion channels which generate stochastic dynamics $\mathcal{D}$ that consists of alternating sequences t_O^i and t_C^j of open and closed times. Using aggregated Markov models, this dynamics is described by transitions between (usually multiple) open and closed states O_m and C_n.

We have first explained how aggregated Markov models can be enumerated i.e. we have shown how the number of different aggregated Markov models for a given number $n = n_O + n_C$ of states can be calculated using Pólya enumeration. The results, which can be found in Table 1, clearly show that the number of aggregated Markov models grows extremely rapidly—for only $n_V = 10$ vertices, we have more than 10 billion models! If we are inclined to interpret each model as a representation of a different biophysical "process", the results in Table 1 are somewhat reduced due to non-identifiability but nevertheless increases quickly with the number of vertices.

The phenomenon of non-identifiability appears somewhat counter-intuitive at first glance—how can a "biophysical process" that is represented by transitions between the open and closed states of a Markov model not be reconstructed from the sequence of open and closed times generated by this "process"? In order to gain a better understanding of this problem, let us consider an open time t_O^i. Due to the presence of multiple open states, it is not clear, by which of the open states O_n the open time t_O^i has been generated—or if, during the time t_O^i, the model has even alternated between multiple open states. This raises the question how much detail of the parameters and/or the structure of an aggregated Markov model can be inferred at all from the dynamics $\mathcal{D}$ i.e. a sequence of open and closed times.

To answer these questions, we have not related models directly to the dynamics $\mathcal{D}$. Instead, we have considered reparametrisations of the infinitesimal generator Q of a given aggregated Markov model. This relies on a classical result by Fredkin et al. (1985); Fredkin and Rice (1986) that the dynamics $\mathcal{D}$ of an aggregated Markov model with n_O open and n_C closed states is characterised by the bivariate distributions $f_{OC}(t_O, t_C)$ and $f_{CO}(t_C, t_O)$. This implies that reparametrising a model Q

so that the distributions $f_{\mathrm{OC}}(t_{\mathrm{O}}, t_{\mathrm{C}})$ and $f_{\mathrm{CO}}(t_{\mathrm{C}}, t_{\mathrm{O}})$ remain unchanged will yield a model $\tilde{Q}$ whose dynamics $\mathcal{D}$ is indistinguishable from the original model Q i.e. Q is *not parameter-identifiable*.

If such a model Q which lacks parameter identifiability is used for modelling ion channels, it will represent the dynamics $\mathcal{D}$ as well as any reparametrised version $\tilde{Q}$ of Q. Thus, the choice of parameters q_{ij} for representing the dynamics $\mathcal{D}$ is not unique—multiple different parameter set (as we have seen, in most cases, infinitely many) represent the dynamics equally well.

If our primary aim is to find a model that reproduces the dynamics $\mathcal{D}$ accurately, this might not be considered a very important problem. Indeed, phase type distributions (Neuts 1978)—which can be interpreted as sojourn time distributions f_{C} of an aggregated Markov model with only one open state—are popular generalisations of the exponential distribution for waiting times. Here, non-identifiability is not a concern because the only role of the states ("phases") is to accurately describe a given data set, not to represent particular "states" of a system. But if our goal is to build aggregated Markov model that represent aspects of the underlying biophysics of the observed dynamics, not being able to unambiguously determine the rates q_{ij} implies that a non-identifiable model does not allow us to gain insight into the transition rates between different biophysical states.

We have investigated the consequences of non-identifiability by considering the fully connected three-state model. For a given parameter set, there usually exists an infinite equivalence class of models. Under certain conditions, this ambiguity could be resolved by reducing the non-identifiable fully-connected model which depends on six rates to either of the parameter-identifiable models COC or CCO which depend on four rates.

However, crucially, this model reduction does not allow us to *rule out* the presence of particular transitions between conformational states that are represented in the fully connected model. Rather, this only demonstrates that given dynamics $\mathcal{D}$ *can* be explained in the absence of some of these transitions between states of the channel protein. But going further, model reduction does not even allow us to distinguish between the models COC and CCO—as we have seen, if a parameter set of the fully connected three-state model can be reduced to the model structure COC it can also be reduced to CCO and vice versa. And despite the fact that the parameters q_{ij} are identifiable for either of the two models, the *model structure $\mathcal{G}$* for models with $n_{\mathrm{O}} = 1$ open and $n_{\mathrm{C}} = 2$ closed states remains non-identifiable—it is not possible to decide if COC or CCO provides a better representation of the dynamics $\mathcal{D}$. This shows that it is not possible to distinguish if the dynamics $\mathcal{D}$ is generated by one "fast" and one "slow" closed state from which the channel can transition to the open state—this mechanism is represented by the model COC. Or, alternatively, via a stepwise process where the channel makes a transition from a closed state C_1 to a state C_2 which primes the channel for entering the open state O_3. The two mechanisms are, obviously, also very different from a biophysical point of view—if we assume, as in Section 3.5—that the transitions between states are regulated by binding sites, the model COC represents a channel with two independent binding sites whereas CCO is based on the assumption of sequential binding.

Interestingly, reducing the non-identifiable fully connected three-state model to an identifiable model with four instead of six rates is not always possible because, for some parameter sets, reparametrising the model would lead to negative rates. In this situation, the non-identifiability cannot be resolved by choosing a particular model, simply because it is not obvious which model to pick as a representative for the infinite sets of equivalent models of the equivalence class. Interpreted from a biophysical point of view, in this case it is not possible to infer, which conformational changes might have generated the observed dynamics $\mathcal{D}$. In the case of the fully connected three-state models, this applied to models for which the sojourn time distribution f_C could not be represented as a mixture of exponential distributions but as a signed mixture of exponentials. This shows that some dynamics $\mathcal{D}$ that aggregated Markov models can generate, cannot be represented with an identifiable model, or, in other words, some dynamics $\mathcal{D}$, in principle, cannot be associated unambiguously with a biophysical mechanism.

In summary, two lessons can be learnt. First, for some parameter sets, the fully connected model can be reduced to the model structures COC and CCO. This means that the dynamics *can* be represented by assuming a simpler, acyclic mechanism. But this does not exclude that the dynamics could equally well be generated by a mechanism where transitions between all states are possible. Also, it is not possible to distinguish between the fundamentally different mechanisms COC and CCO. Second, the fully connected three-state model can generate sojourn time distributions based on a signed mixture of exponential whose densities show local maxima and minima rather than the monotonously decreasing densities obtained from a "normal" mixture of exponential distributions (where all coefficients of the exponentials are positive and form a finite probability distribution). These sojourn time distributions cannot be represented so that the model is parameter-identifiable so that these dynamics cannot be associated with transitions between different conformational states of the channel protein.

It has been suggested that the problem of identifiability of model structure (i.e. of the underlying biophysical mechanism) might be addressed by considering multiple data sets. We have investigated the question if the two alternative three-state models COC and CCO could be distinguished when the dependency of a channel on the concentration c of a ligand is considered. Starting from models based on particular assumptions for different ligand binding sites, we have investigated how the ligand dependencies differ in the transformed model CCO after reparametrising the model COC. For some models, our results show that some transitions in the transformed model CCO are enzyme kinetics whereas in the original model COC, mass action was assumed. This does not help to distinguish COC and CCO because alongside mass action kinetics, Michaelis-Menten terms (or other Hill functions) are common models of ligand binding in ion channel modelling. A clearer hint that dynamics $\mathcal{D}$ could be better described by the COC model than the CCO model, might be the emergence of ligand-dependent transitions where they would normally not be expected—the most striking example is the case of the COC model with two activating binding sites, see Section 3.5.1: here, the mass action rates $q_{13}(c)$ and $q_{23}(c)$ connecting the closed states C_1 and C_2 to the open state O_3 in the model COC translate to analogous rates $q_{12}(c)$ and $q_{23}(c)$ in the transition from closed state C_1 via C_2 to the open state O_3 in the model CCO. But

the emergence of a mass action rate $q_{21}(c)$ in the transition from C_2 to C_1 is unexpected and would unlikely be chosen as such if the model had been developed based on mechanistic assumptions. It remains to be seen if criteria like this can be exploited in practice when comparing the fits of equivalent ion channel models to the same data set.

Having explored the non-identifiability of aggregated Markov models, we will reflect on implications for modelling ion channels and indicate how mechanistic data-driven models can nevertheless be developed under these circumstances. Beyond the sufficient condition of $2n_O n_C$ for the maximum number of rate constants of an aggregated Markov model introduced by Fredkin et al. (1985); Fredkin and Rice (1986), to the best of our knowledge, no other criteria are available that can be applied easily to decide if a given Markov model is identifiable. If it is unknown if a given model is identifiable, indirect information can be gained by using approaches that investigate the uncertainties of parameters. We have suggested specifically that Markov chain Monte Carlo (MCMC) can be useful for deciding if a model could be non-identifiable (Siekmann et al. 2012). Alternatively, profile likelihood approaches have been applied to a wide range of models to assess identifiability (Bates and Watts 1988; Raue et al. 2009; Kreutz et al. 2012, 2013; Simpson and Maclaren 2023; Ciocanel et al. 2024; Plank and Simpson 2024) although, to the best of our knowledge, they have not been applied specifically to aggregated Markov models.

An approach that attempts to address both the lack of parameter identifiability as well as non-identifiability of model structure is the use of *canonical forms*. Canonical forms as those proposed by Bauer et al. (1987); Kienker (1989) and Larget (1998); Bruno et al. (2005); Flomenbom and Silbey (2006) are model structures that are on the one hand parameter identifiable and on the other hand, provide representatives for each of the different model structures that exist for a given number of open and closed states. Restricting the set of models to be considered to representatives of an equivalence classes of models makes the process of model selection more efficient because it prevents the modeller from comparing fits of equivalent models (such as the models CCO and COC investigated in detail in this study) which, in theory, should show identical performance when fitted to the same data. Although canonical forms solve the statistical problems related to non-identifiability when it comes to fitting aggregated Markov models to data, modellers are restricted to the model structures defined by the canonical forms which constrains their freedom of representing biophysical mechanisms. A more severe problem is that some data sets might only be represented by physically unrealistic models, for example, the *manifest interconductance rank (MIR)* form proposed by Bruno et al. (2005) as well as the BKU form (Bauer et al. 1987; Bruno et al. 2005) might only be able to model some data sets if some rates are allowed to be negative, similar to the example presented in Section 3.4. Nevertheless, the MIR form by Bruno et al. (2005) allows for a refined representation of the equivalence classes of aggregated Markov models because it considers the "interconductance rank" p_{OC} i.e. the rank of the transition matrices Q_{CO} and Q_{OC} which consist of the rates connecting open and closed states. In MIR form, the number of transitions between open and closed states is chosen to coincide with the rank of Q_{CO} and Q_{OC}. The MIR form therefore depends on $2p_{OC}(n_O + n_C - p_{OC})$ param-

eters, consistent with the refined upper bound for the maximum number of parameters derived in Fredkin and Rice (1986).

It remains a challenging problem to design models that represent the observed dynamics $\mathcal{D}$ of an ion channel but also capture biophysical processes such as conformational changes. Designing models based on detailed knowledge of activating and inhibitory binding sites and other molecular properties of the ion channel leads to models with complex structures consisting of a large number of states and many parameters. Thus, this approach is fraught with problems related to non-identifiability, or, even more simply, over-parametrisation. Building models that mimic aspects of the molecular structure of ion channels is based on the hope that the parameters of these models will reflect the transition rates between biophysical states of the ion channel and thus provide insights into the time scales of conformational changes.

We would like to contrast this with alternative approaches that provide more direct insight into the time scales of conformational changes by rigorous statistical analysis of the dynamics $\mathcal{D}$. Modal gating is a phenomenon that describes ion channels switching between different dynamical patterns characterised by different levels of activity (i.e. for example different levels of open probability). These modes form a limited repertoire of dynamical patterns between which the ion channel alternates instantaneously. Thus, from a mathematical point of view, modal gating is an example of dynamics that exhibits two clearly different time scales. The "fast" dynamics is characterised by different modes that are associated with particular dynamical patterns. On the "slow" time scale the ion channel switches between these modes.

Modal gating has been investigated statistically by Ionescu et al. (2007); Siekmann et al. (2014). Both have developed methods which enable us to quantitatively infer the time scales of switching between modes as well as characterise the dynamics of individual modes. It is well-established that modes are manifestations of different conformational states in the dynamics of an ion channel, see, in particular, the study Chakrapani et al. (2011) as well as a wealth of additional references reviewed in the Discussion of Siekmann et al. (2014). Thus, statistical analysis of modal gating enables us to infer the dynamics of conformational changes of the ion channel by associating modes with different conformational states of the ion channel. The importance of modal gating for the modelling of ion channels is increasingly recognised—modal gating dynamics was included in Ullah et al. (2012) as one of multiple data sources. Siekmann et al. (2012) and Bicknell and Goodhill (2016) built models whose structures were designed based on modal gating as the underlying construction principle and Siekmann et al. (2016) proposed a structure specifically for representing modal gating as a hierarchical process—the hierarchical Markov model combines a Markov model that represents the switching between different modes with models for the dynamics of the individual modes to a model that accounts for both switching between modes as well as the dynamics within modes. Due to the close relationships of modes and conformational states, the states of the hierarchical Markov model can be interpreted to represent conformational changes, similar to models based on certain assumptions on biophysical processes such as ligand binding. But in contrast to these models, in the hierarchical Markov model, the rates between different conformational states can be parameterised based on a rigorous statistical analysis of the transitions between modes observed in the data.

Additional insight into both the dynamics as well as the molecular structure of ion channels can be gained from data that characterises the latency of an ion channel i.e. the delayed response of an ion channel to changes in ligand concentrations. Hawker et al. (2025) developed a method for extending an existing model whose ligand dependency was parametrised using multiple data sets at constant concentrations c by integrating additional data that investigated the response of the channel to changes of the ligand concentration. The biophysical significance of this model can best be understood by considering the transition from a ligand concentration c_1 to a ligand concentration c_2 where for concentration c_1 the channel protein is in conformation A with a high probability whereas for concentration c_2 the channel is most likely in different conformational state B. When instantaneously switching from c_1 to c_2 the channel cannot immediately adjust to the new ligand concentration, instead it transitions from A to B with a delay. This delay is represented in the model by introducing an integral term that averages the ligand concentration over a certain finite time interval. Thus, instead of an immediate switch the integral introduces a gradual transition from c_1 to c_2 and instead of an immediate "jump" the transition from conformation A to conformation B comes with a delay.

In summary, our study has demonstrated that non-identifiability poses difficult challenges for developing models that represent both the dynamics $\mathcal{D}$ as well as the biophysics of an ion channel by identifying individual states of a Markov model with conformational states of the channel protein. But we have presented some alternative approaches for developing models that represent conformational changes underlying the opening and closing of an ion channel by integrating additional data. By giving this detailed introduction into the complex phenomenon of non-identifiability we hope to facilitate the task of building mechanistic data-driven models of ion channels and, more general, taking advantage of the framework of aggregated Markov models for other applications.

Data Availability This study has no associated data.

References

Bauer RJ, Bowman BF, Kenyon JL (1987) Theory of the kinetic analysis of patch-clamp data. Biophys J 52(6):961–978. https://doi.org/10.1016/S0006-3495(87)83289-7

Bicknell BA, Goodhill GJ (2016) Emergence of ion channel modal gating from independent subunit kinetics. Proc Natl Acad Sci 113(36):5288–5297. https://doi.org/10.1073/pnas.1604090113

Bates, D.M., Watts, D.G.: Nonlinear Regression Analysis and Its Applications. Wiley series in probability and mathematical statistics. Applied probability and statistics. John Wiley & Sons Inc., Toronto (1988). https://doi.org/10.1002/9780470316757

Bruno WJ, Yang J, Pearson JE (2005) Using independent open-to-closed transitions to simplify aggregated Markov models for ion channel gating kinetics. Proceedings of the National Academy of Science of the United States of America 102(16):6326–6331. https://doi.org/10.1073/pnas.0409110102

Chakrapani S, Cordero-Morales JF, Jogini V, Pan AC, Cortes DM, Roux B, Perozo E (2011) On the structural basis of modal gating behaviour in K^+ channels. Nat Struct Mol Biol 18(1):67–75. https://doi.org/10.1083/nsmb.1986

Ciocanel M-V, Ding L, Mastromatteo L, Reichheld S, Cabral S, Mowry K, Sandstede B (2024) Parameter identifiability in pde models of fluorescence recovery after photobleaching. Bull Math Biol 86(4):36. https://doi.org/10.1007/s11538-024-01266-4

Colquhoun D, Hawkes AG (1981) On the stochastic properties of single ion channels. Proceedings of the Royal Society of London B 211:205–235. https://doi.org/10.1098/rspb.1981.0003

De Young GW, Keizer J (1992) A single-pool inositol 1,4,5-trisphosphate-receptor-based model for agonist-stimulated oscillations in Ca^{2+} concentration. Proc Natl Acad Sci 89(20):9895–9899

Fredkin, D.R., Montal, M., Rice, J.A.: Identification of aggregated Markovian models: Application to the nicotinic acetylcholine receptor. In: Cam, L.M.L., Olshen, R.A. (eds.) Proceedings of the Berkeley Conference in Honor of Jerzy Neyman and Jack Kiefer, vol. 1, pp. 269–289. Wadsworth, Belmont, CA (1985)

Fredkin DR, Rice JA (1986) On aggregated Markov processes. J Appl Probab 23(1):208–214

Flomenbom O, Silbey RJ (2006) Utilizing the information content in two-state trajectories. Proc Natl Acad Sci USA 103(29):10907–10910. https://doi.org/10.1073/pnas.0604546103

Hawker M, Cao P, Kelly RA, Sneyd J, Siekmann I (2025) A ca^{2+} puff model based on integrodifferential equations. J Math Biol 90(4):43. https://doi.org/10.1007/s00285-025-02202-3

Harary F, Palmer EM (1973) Graphical Enumeration. Academic Press, New York and London

Ito, H., Amari, S., Kobayashi, K.: Identifiability of hidden markov information-sources and their minimum degrees of freedom. IEEE Transactions on Information Theory 38(2, 1), 324–333 (1992) https://doi.org/10.1109/18.119690

Ionescu L, White C, Cheung K-H, Shuai J, Parker I, Pearson JE, Foskett JK, Mak D-OD (2007) Mode switching is the major mechanism of ligand regulation of InsP$_3$ receptor calcium release channels. J Gen Physiol 130(6):631–645

Kienker P (1989) Equivalence of aggregated Markov models of ion-channel gating. Proceedings of the Royal Society of London B 236:269–309

Kreutz C, Raue A, Kaschek D, Timmer J (2013) Profile likelihood in systems biology. FEBS J 280(11):2564–2571. https://doi.org/10.1111/febs.12276

Kreutz C, Raue A, Timmer J (2012) Likelihood based observability analysis and confidence intervals for predictions of dynamic models. BMC Syst Biol 6(1):120. https://doi.org/10.1186/1752-0509-6-120

Larget B (1998) A canonical representation for aggregated Markov processes. J Appl Probab 35(2):313–324. https://doi.org/10.1239/jap/1032192850

Mak D-OD, Pearson JE, Loong KPC, Datta S, Fernández-Mongil M, Foskett JK (2007) Rapid ligand-regulated gating kinetics of single inositol 1,4,5-trisphosphate receptor ca^{2+} release channels. EMBO Rep 8(11):1044–1051. https://doi.org/10.1038/sj.embor.7401087

Neuts, M.F.: Renewal processes of phase type. Naval Research Logistics 25(3), 445–454 (1978). cited By 32

Pólya, G.: Kombinatorische Anzahlbestimmungen f r Gruppen, Graphen und chemische Verbindungen. Acta Mathematica 68(none), 145–254 (1937) https://doi.org/10.1007/BF02546665

Plank MJ, Simpson MJ (2024) Structured methods for parameter inference and uncertainty quantification for mechanistic models in the life sciences. Royal Society Open Science 11(8):240733. https://doi.org/10.1098/rsos.240733

Riddell, R.J.: Contributions to the theory of condensation. PhD thesis, University of Michigan, Ann Arbor (1951)

Raue A, Kreutz C, Maiwald T, Bachmann J, Schilling M, Klingmüller U, Timmer J (2009) Structural and practical identifiability analysis of partially observed dynamical models by exploiting the profile likelihood. Bioinformatics 25(15):1923–1929

Rydén T (1996) On identifiability and order of continuous-time aggregated markov chains, markov-modulated poisson processes, and phase-type distributions. J Appl Probab 33(3):640–653 (**Accessed 2025-09-10**)

Siekmann I, Crampin EJ, Sneyd J (2012) MCMC can detect non-identifiable models. Biophys J 103(11):1275–1286. https://doi.org/10.1016/j.bpj.2012.10.024

Siekmann, I., Cao, P., Sneyd, J., Crampin, E.J.: Data-driven modelling of the inositol trisphosphate receptor (IP_3R) and its role in calcium induced calcium release (CICR). In: Pittà, M.D., Berry, H. (eds.) Computational Glioscience, pp. 39–68. Springer (2019). Chap. 2. https://doi.org/10.1007/978-3-030-00817-8_2

Siekmann I, Fackrell M, Crampin EJ, Taylor P (2016) Modelling modal gating of ion channels with hierarchical markov models. Proceedings of the Royal Society of London A 472:20160122. https://doi.org/10.1098/rspa.2016.0122

Simpson MJ, Maclaren OJ (2023) Profile-wise analysis: A profile likelihood-based workflow for identifiability analysis, estimation, and prediction with mechanistic mathematical models. PLoS Comput Biol 19(9):1–31. https://doi.org/10.1371/journal.pcbi.1011515

Siekmann I, Sneyd J, Crampin EJ (2014) Statistical analysis of modal gating in ion channels. Proceedings of the Royal Society of London A 470(2166):20140030. https://doi.org/10.1098/rspa.2014.0030

Siekmann I, Wagner LE II, Yule D, Crampin EJ, Sneyd J (2012) A kinetic model of type I and type II IP_3R accounting for mode changes. Biophys J 103(4):658–668. https://doi.org/10.1016/j.bpj.2012.07.016

Ullah G, Mak D-OD, Pearson JE (2012) A data-driven model of a modal gated ion channel: The inositol 1,4,5-trisphosphate receptor in insect Sf9 cells. J Gen Physiol 140(2):159–173. https://doi.org/10.1085/jgp.201110753